EFFECTS OF OUTLET TURBULENCE INTENSITY UPON AIR DISTRIBUTION

by

SUNG-NAN HSU

B. S., Taiwan Cheng Kung University, 1967

A MASTER'S THESIS

submitted in partial fulfillment of the

requirements for the degree

MASTER OF SCIENCE

Department of Mechanical Engineering

KANSAS STATE UNIVERSITY
Manhattan, Kansas

1973

Approved by:

Ralph G. Nevins
Major Professor

TABLE OF CONTENTS

LIST OF TABLES

LIST OF FIGURES

Figure | Page

NOMENCLATURE

C_d - Discharge coefficient of a jet

D - Outlet diameter of a jet, in.

E_b - Bridge output voltage of a hot-wire anemometer, volt

K - Proportionality constant

ℓ_t - The Lagrangian scale of turbulence

P - Static pressure, psi

$\bar{P}$ - Mean static pressure, psi

P' - Fluctuating static pressure, psi

R - Correlation coefficient

R_f - The proportion of free area to gross area of a jet outlet

T - Temperature, ^oF

$\bar{T}$ - Mean temperature, ^oF

t - Time, sec

T_o - Temperature at the outlet of the jet, ^oF

T_e - Temperature at the exhaust of the test chamber, ^oF

u, v, and w - Time-average velocities in the directions of x, y, and z respectively, ft/min

$\bar{u}$, $\bar{v}$, and $\bar{w}$ - Components of the mean velocity in the directions of x, y, and z respectively, ft/min

$\bar{u'}$ - Mean value of the velocity fluctuation in x direction, ft/min

$\overline{u'^2}$, $\overline{v'^2}$, and $\overline{w'^2}$ - Mean square of the velocity fluctuations in x, y, and z directions respectively, $(ft/min)^2$

$\overline{u'v'}$, $\overline{v'w'}$, and $\overline{u'w'}$ - Turbulence shear components, $(ft/min)^2$

V_o - Jet outlet velocity, ft/min

V_c - Center-line velocity in a jet, ft/min

x - The distance away from a jet outlet, in

ϵ - Turbulence intensity, per cent

ϵ_o - Turbulence intensity at the outlet of a jet, per cent

INTRODUCTION

The distribution of air in an occupied space is a very important but complex problem. Major contributions to the understanding of jets and to air distribution in the occupied space for various outlet conditions have been made through ASHRAE's long-range research program.

However, little if any data have existed concerning the effects of a change in outlet turbulence intensity, all other factors remaining unchanged, upon the distribution in the occupied space.

For this study, a model space 12in x 12in x 44in was used with two sets of experiments: one with a single outlet jet, and the other with multiple jets. For each value of outlet intensity of turbulence, measurements and observations were made of:

1. outlet velocities, turbulence intensities, and flow rates.
2. centerline velocities, turbulence intensities, and terminal velocities in the jet.
3. air velocities and turbulence intensities in the occupied space.
4. general air flow patterns in the test chamber.

BASIC CONCEPTS OF TURBULENCE INTENSITIES

Turbulent fluid motion is an irregular condition of flow in which the various quantities show a random variation with time and space coordinates, so that statistically distinct average values can be discerned.

Intensity

For steady, incompressible, constant viscosity fluids, we have

velocity component in the x-direction $u = \bar{u} + u'$

velocity component in the y-direction $v = \bar{v} + v'$

velocity component in the z-direction $w = \bar{w} + w'$

static pressure $P = \bar{P} + P'$

temperature $T = \bar{T} + T'$

with barred letters for mean quantities and primed letters for fluctuation components.

For an isothermal constant-static-pressure, incompressible, unidirectional flow-stream, the practical significance of turbulent fluctuations may be demonstrated by considering only the velocity fluctutions.

For x-directional flow, when averaged over some finite time interval, by rule of averages, the fluctuating components are equal to zero.

$$\overline{u'} = \frac{1}{t}\int_0^t u'dt = 0$$

while the square of the velocity fluctuations $\overline{u'^2}$, $\overline{v'^2}$, $\overline{w'^2}$ and the turbulent shear components $\overline{u'v'}$, $\overline{v'w'}$ and $\overline{u'w'}$ are finite.

The mean square of the velocity fluctuations is defined as

$$\overline{u'^2} = \frac{1}{t} \int_0^t u'^2 \, dt$$

and the root mean square of the velocity fluctuations is $\sqrt{\overline{u'^2}}$. The intensity of the turbulent fluctuations is defined as

$$\text{Intensity} = \frac{\sqrt{\overline{u'^2}}}{\overline{u}}$$

Intensity is also expressed in terms of a percentage of the mean value; i.e., it is given as $100 \sqrt{\overline{u'^2}}/\overline{u}$. Similar definitions and relations may be obtained for y-direction and z-direction.

Correlation

At a given point, correlation coefficient between u′ and v′ is defined as

$$R = \frac{\overline{u'v'}}{\sqrt{\overline{u'^2}} \sqrt{\overline{v'^2}}}$$

The magnitude of R may vary between 0 and 1 inclusive. If R = 0, then the fluctuations u′ and v′ are completely unrelated. If R = 1, then u′ and v′ are uniquely interrelated.

Scale

Using the correlation coefficients, the Lagrangian scale of turbulence is defined as

$$\ell_t = \sqrt{\overline{u'^2}} \int_0^\infty R_t dt$$

where R_t is defined by $R_t = \dfrac{\overline{u_t' \, u_{t+\Delta t}}}{\overline{u'^2}}$, subscript t represents the time.

The "scale" of turbulence can be explained as a probability-weighted mean distance of particle travel during the time interval required for R_t to become zero. Scale magnitudes are usually less than one inch in engineering problems.

Isotropy

Isotropy is that condition wherein the intensity components and scales in all directions are equal at any given point. Isotropy also means that the fluctuations are perfectly random, with the result that there is no relation between components of the fluctuation in different directions: i.e.,

$$\overline{u'v'} = \overline{v'w'} = \overline{u'w'} = 0$$

As a practical approximation, the theories of isotropic turbulence have been extended to the utmost for engineering expediency, because non-isotropic turbulence in engineering flow systems has a strong natural tendency to become isotropic.[2]

THIS BOOK CONTAINS NUMEROUS PAGES WITH DIAGRAMS THAT ARE CROOKED COMPARED TO THE REST OF THE INFORMATION ON THE PAGE.

THIS IS AS RECEIVED FROM CUSTOMER.

BASIC CHARACTERISTICS OF JETS

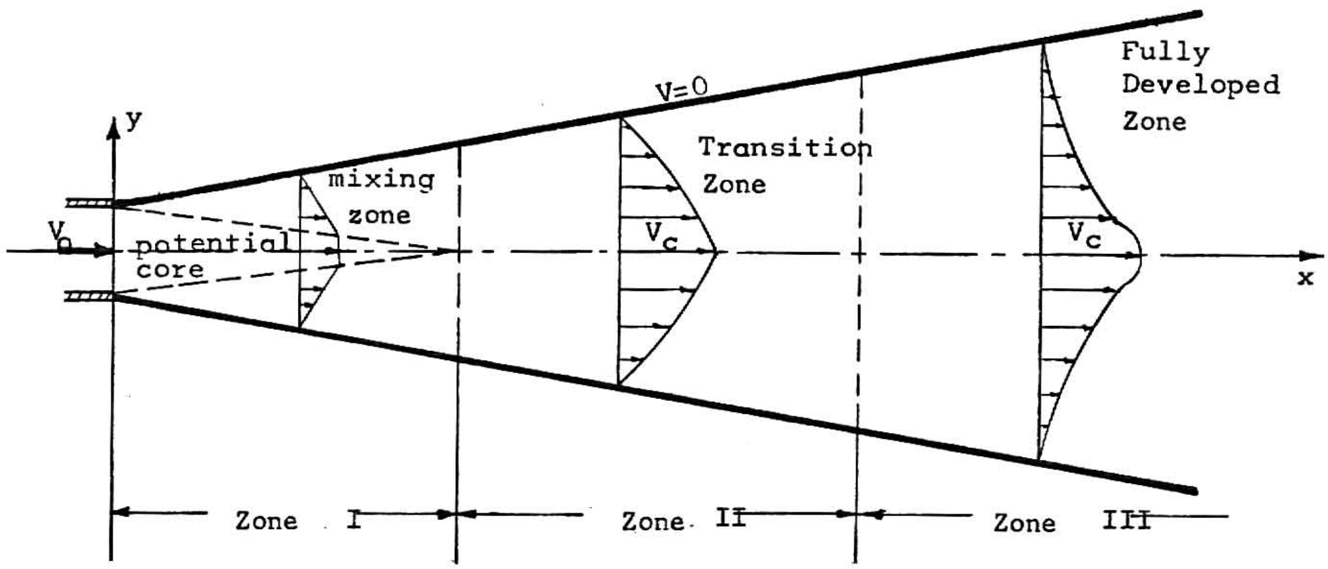

Fig. 1 Shape of Single Jet

There are three major zones to be recognized along the direction of flow of a free jet as shown in Fig. 1.

Zone 1: a short zone, two to six diameters from the outlet face in which a core of fluid of uniform velocity exists.

Zone 2: a transition region that usually extends to 8 or 10 diameters, the maximum velocity in this zone may vary inversely as the square root of the distance from the outlet and in which the cross-stream profile is usually recognized as being hyperbolic.

Zone 3: The fully developed region or the principal zone is achieved at about 10 diameters downstream. Maximum axial or centerline velocity is inversely proportional to the axial distance, which can be described by the equation[6]

$$\frac{V_c}{V_o \sqrt{C_d R_f}} = K \frac{D}{X}$$

where K is a proportionality constant, C_d is the discharge coefficient of the outlet, R_f is the proportion of free area to gross area of the outlet. The Cross-stream velocity profile resembles a typical probability curve(or an error function). This is the most important zone for air distribution.

For multiple jets, or air streams discharged from perforated panels, it has been shown[4,5] that immediately after the separate jets leave the outlet a contraction takes place and the separate jets attain their greatest velocity in the section K—K, Fig. 2, after which the velocity is diminished through entrainment of surrounding air; the separate jets unite quickly into one homogeneous jet, and then behave in a manner similar to a free jet from a single outlet.

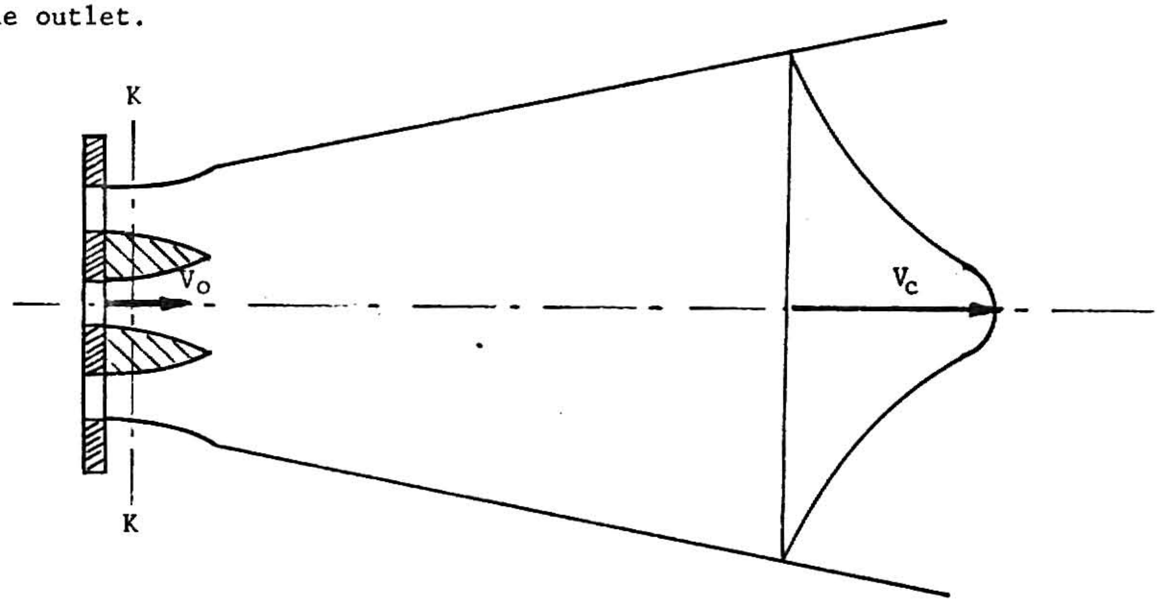

Fig. 2 Shape of Multiple Jets

TEST EQUIPMENT

General Description

The general components of the equipment used in this investigation are shown in Fig. 3. The unit consisted of a plenum, a manometer, a test chamber, measuring instruments, and a one inch diameter brass tube with 3/16 inch diameter nozzle and turbulence promotor.

The main jet was directed from a plenum supplied by compressed air and controlled by a regulator. The radially-inward air jets for the turbulence promotor were supplied directly by compressed air and controlled by another regulator. The flow rate for the main jet was measured by the pressure drop across the 3/16 inch nozzle. The flow rate through the turbulence promotor was estimated by connecting the supply tube of the turbulence promotor directly to the plenum. The flow through the nozzle was then assumed to be the total flow and related the main flow and the flow through the turbulence promotor by the equation

$$Q_t = Q_m + Q_r$$

where Q_t = the total flow rate, cfm

Q_m = the flow rate for the main jet, cfm

Q_r = the flow rate through the turbulence promotor, cfm

The test chamber (12x12x44 in) was made with a wooden floor and rear side, and with transparent plastic for the other sides. Air flow patterns were observed through the use of titanium tetra-chloride ($TiCl_4$) smoke.

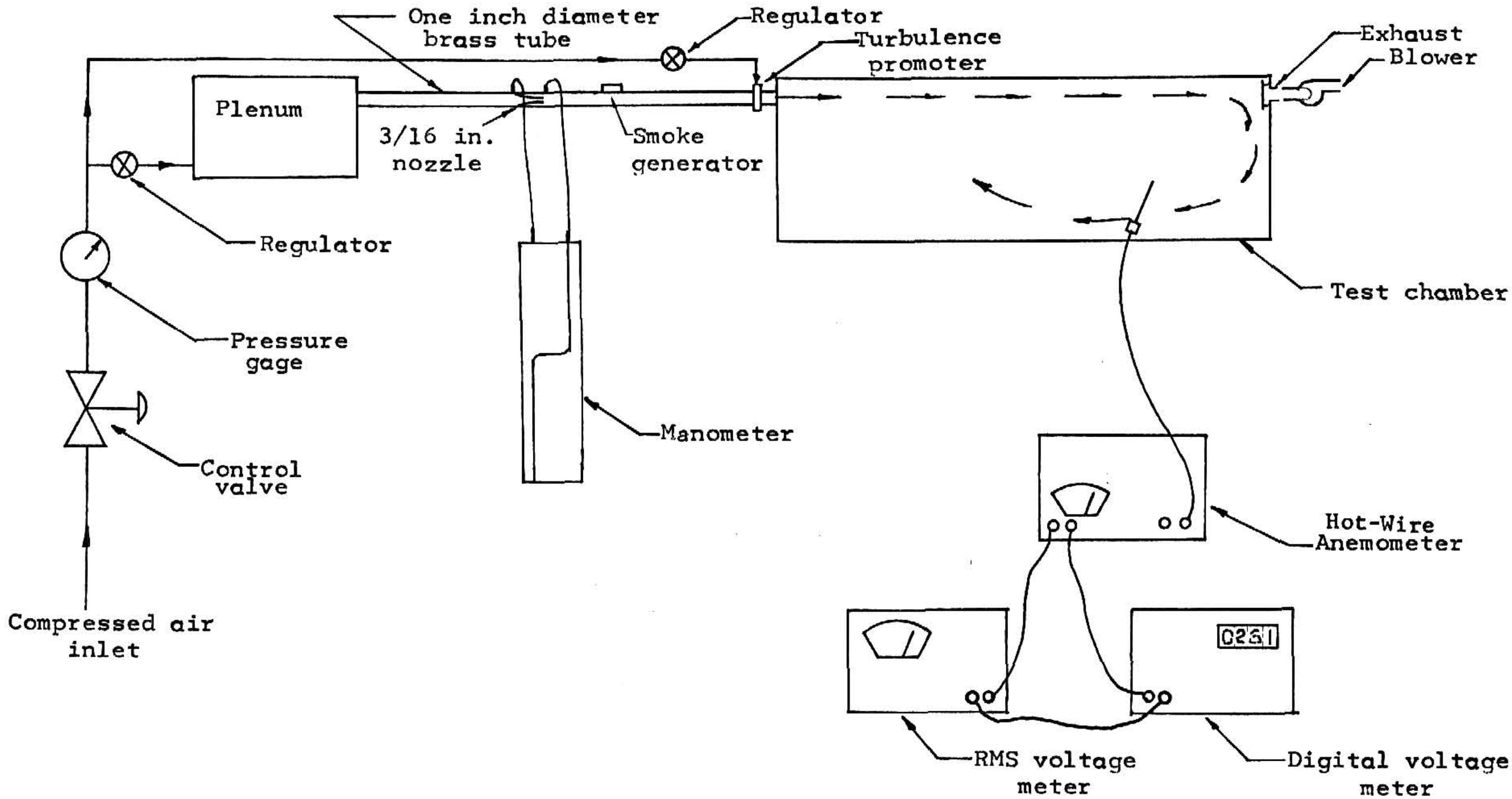

Fig. 3 Schematic Diagram of the Equipment Used in the Present Investigation

Changing of the Outlet Turbulence Intensity

A main experimental problem was to change outlet turbulence intensity without altering the mean center-line velocity. Any device used for changing turbulence level such as baffles, grids, screens and radially-inward air jets, etc. dissipated the available mechanical energy of the flow, thus decreased the outlet velocity. For the present tests of isothermal jets, keeping the mean outlet center-line velocity constant was considered to be more important than maintaining the flow rate for different outlet turbulence intensities.

The outlet turbulence intensities were controlled by means of common window screens and a turbulence promoter. Tubes with different inner surface roughness were tested but failed to produce a significant change of outlet turbulence level, since probably the effect of the surface roughness was merely to generate turbulence within a very thin boundary layer. Keeping the mean center-line velocity at the outlet with a constant rate of 515 fpm for the one inch diameter free-open jet, the turbulence intensity of the unmodified outlet was about 6%; fine screens decreased the intensity to 3%, while the turbulence promotor increased the intensity up to 40%.

The details of the turbulence promotor are shown in Fig. 4. The turbulence intensity was propotional to the amount of air flowing through the radially-inward jets. Screens were used to prevent disturbance of the outlet velocity distribution.

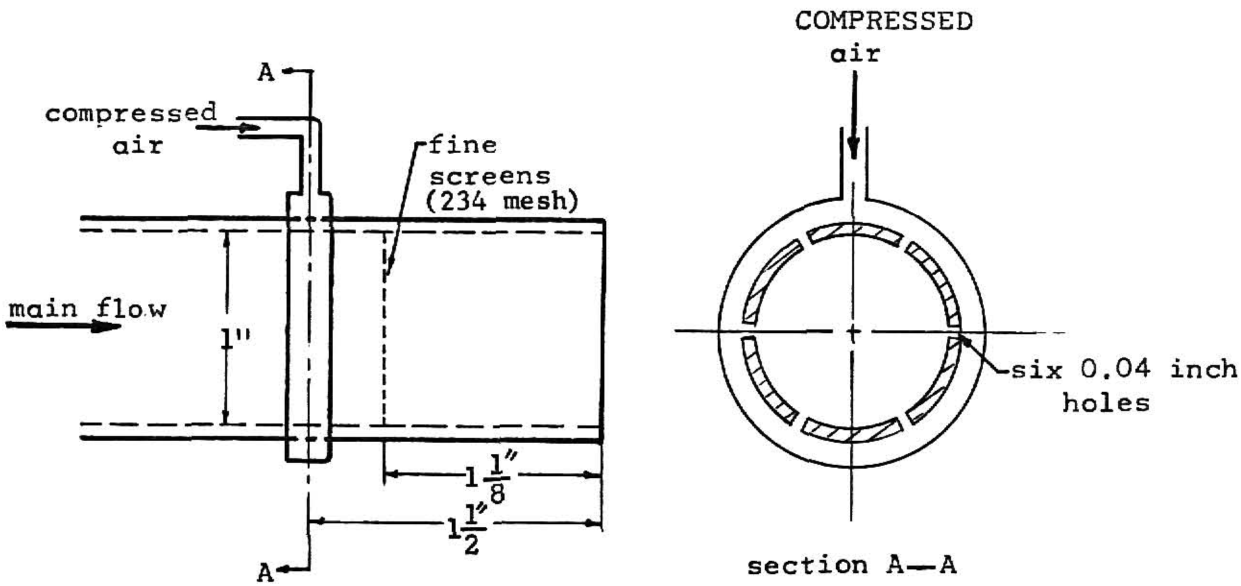

Fig. 4 Turbulence Promotor

INSTRUMENTATION

Measurement of Mean Velocities

A brief description of the equipment is given because an understanding of the performance of the equipment plays a vital part in the interpretation of the measurements obtained. A hot-wire anemometer used for the measurements was a "constant temperature" instrument where the wire is kept at a constant resistance in a Wheatstone bridge circuit fed in a closed loop by a high transconductance d. c. amplifier. Instantaneous velocities are measured in a fluid stream through the stream's instantaneous cooling of the very thin electrically-heated wire filament. The anemometer can be conveniently calibrated in any steady flow. A typical calibration curve, which appears non-linear, is shown in Fig. 5. A good approximation for the relation[7] is

$$E_b \propto u^{\frac{1}{4}} \quad , \qquad 30 \text{ ft/sec} < u < 500 \text{ ft/sec}$$

where E_b is the voltage output and u the mean velocity. The hot-wire calibration fitted this relation to within $\pm 2\%$. But the relation between the squared bridge output voltage ($E_b{}^2$) and the square root of the fluid velocity ($\sqrt{V}$) is linear to within $\pm 5\%$ as shown in Fig. 6.

Measurement of Turbulence Intensities

A combination of the hot-wire anemometer and R.M.S.(root mean squared) voltage meter was used for measuring the turbulence intensities. The principle underlying the R. M. S. voltmeter is based on the definition of the actual root-mean-squared value of a fluctuating voltage, E_b':

$$E'_{b_{RMS}} = \sqrt{\frac{1}{T}\int_0^T E_b'^2 \, dt}$$

where E_b' = the fluctuation of input voltage, E_b

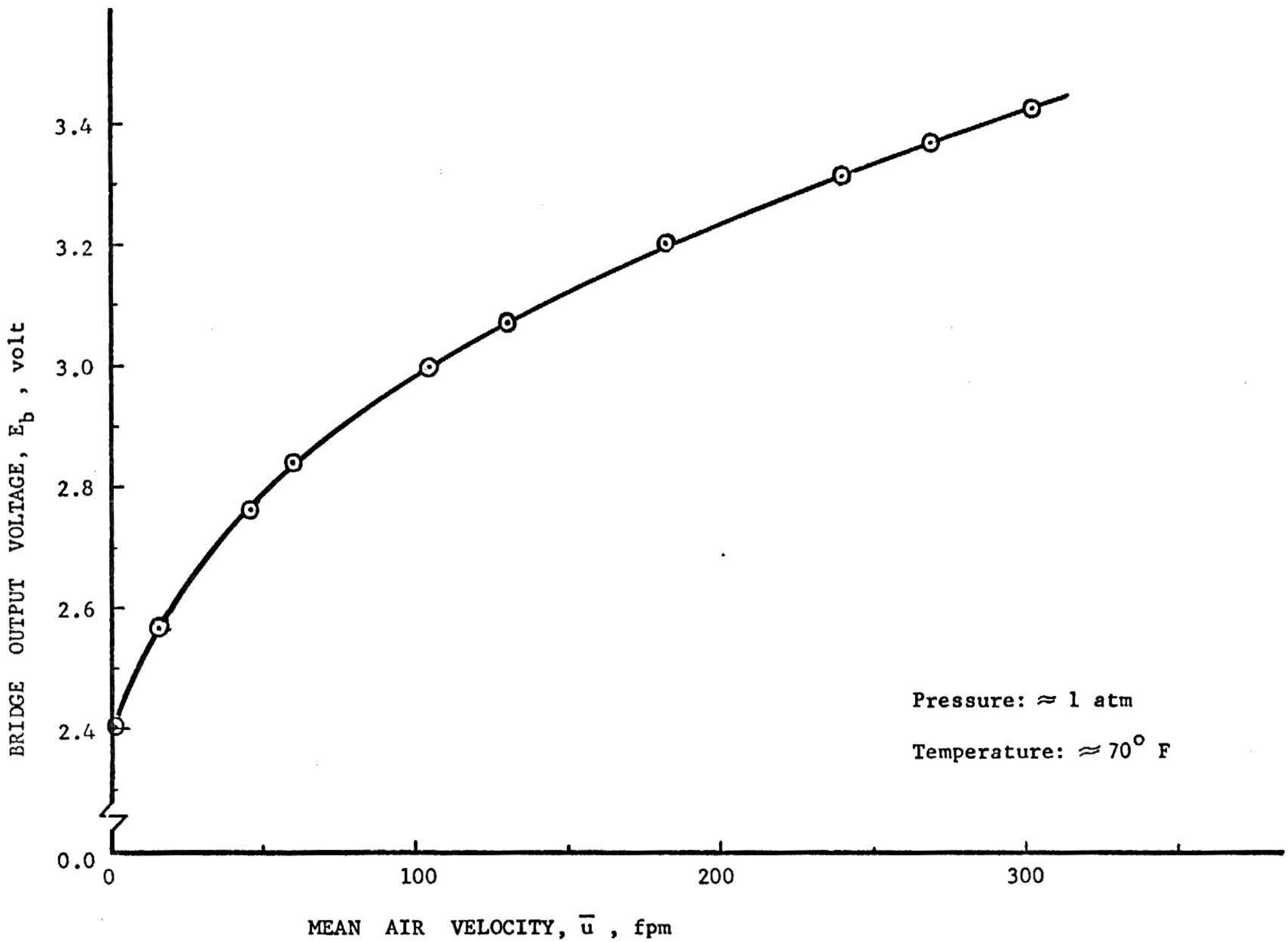

Fig. 5 CALIBRATION CURVE OF A HOT-WIRE ANEMOMETER

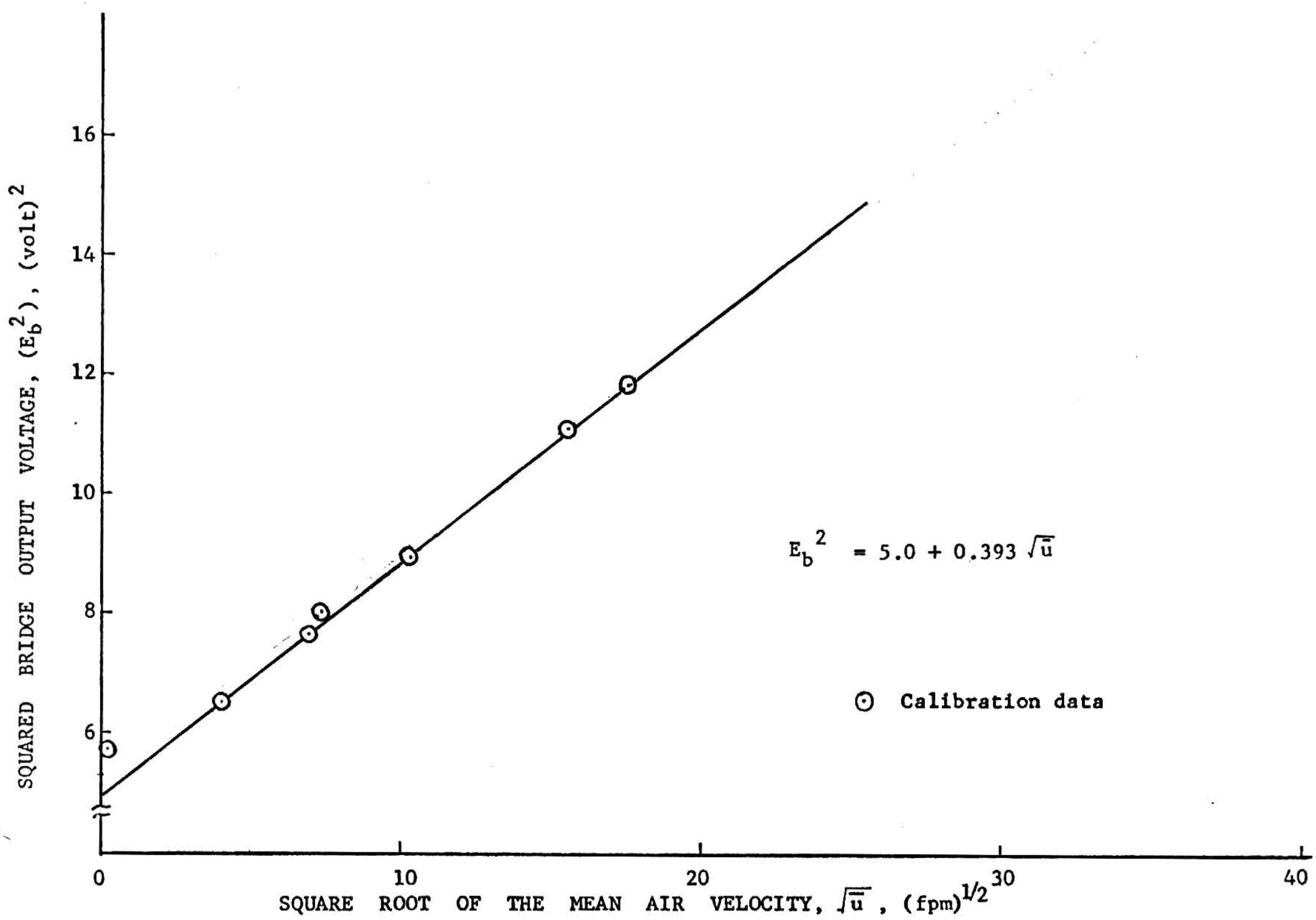

Fig. 6 APPROXIMATE LINEAR RELATION BETWEEN E_b^2 AND $\sqrt{\bar{u}}$

E_b = the output voltage of the hot-wire anemometer

T = time constant

$E_{b\,RMS}'$ = root-mean-squared value of E_b'

Because of the non-linear relation between the anemometer output voltage (E_b) and the mean air velocity ($\bar{u}$), a linearization of E_b and $\bar{u}$ was made as follows:

$$\sqrt{\overline{E_b'^2}}\Big]_p = E_b'\Big]_p = \frac{d\,E_b}{d\,\bar{u}}\Big]_p \cdot u'\Big]_p = \frac{d\,E_b}{d\,\bar{u}}\Big]_p \cdot \sqrt{\overline{u'^2}}\Big]_p$$

where subscript p represents any refrence point on the calibration curve in Fig. 5.

Hence, the turbulence intensity can be found in relation to the R.M.S. voltage, the slope of calibration curve, and the mean air velocity:

$$\epsilon \equiv \frac{\sqrt{\overline{u'^2}}\Big|_p}{\bar{u}\Big]_p} = \frac{\sqrt{\overline{E_b'^2}}\Big]_p}{\frac{d\,E_b}{d\,\bar{u}}\Big]_p \cdot \bar{u}\Big]_p} = \frac{V_{RMS}\Big|_p}{M\Big]_p\ \bar{u}\Big]_p} \qquad (\ a\ )$$

where $V_{RMS} = \sqrt{\overline{E_b'^2}}$ = readings from the R.M.S. voltmeter

$M = \frac{d\,E_b}{d\,\bar{u}}$ = the slope of the bridge DC voltage versus the mean flow velocity in the calibration curve, volts/fpm

Equation (a) can also be written as

$$\text{percentage of turbulence} = \frac{100 \cdot V_{RMS}}{M \cdot \bar{u}} \qquad (\ b\ )$$

If, however, we may assume the existance of a linear relationship between the squared bridge output voltage (E_b^2) and the square root of the fluid velocity ($\sqrt{\bar{u}}$), as verified by L. V. King[17] and others (see Fig. 6). Then the turbulence intensity can be calculated without it being necessary to have the calibration curve[17]. This is shown as follows:

The linear relationship

$$E_b^2 = E_{b_o}^2 + b \cdot \sqrt{\bar{u}} \qquad (c)$$

where E_{b_o} denotes the bridge voltage at zero flow velocity and $b = \frac{d\,E_b^2}{d\sqrt{\bar{u}}}$ the slope of the linear equation (c).

Differentiating equation (c) with respect to the mean flow velocity $\bar{u}$, gives:

$$2\,E_b\,\frac{dE_b}{d\,\bar{u}} = b \cdot \frac{1}{2\sqrt{\bar{u}}}$$

or,

$$\frac{d\,E_b}{d\,\bar{u}} = \frac{b}{4\,E_b\sqrt{\bar{u}}} \qquad (d)$$

from (c),

$$\sqrt{\bar{u}} = \frac{E_b^2 - E_{b_o}^2}{b} \qquad (e)$$

From (d) and (e), we have

$$M \cdot \bar{u} = \frac{d\,E_b}{d\,\bar{u}} \cdot \bar{u} = \frac{b}{4\,E_b\sqrt{\bar{u}}}\,\bar{u} = \frac{b\sqrt{\bar{u}}}{4\,E_b} = \frac{E_b^2 - E_{b_o}^2}{4\,E_b}$$

Hence,

$$\text{percentage of turbulence intensity} = 100 \cdot V_{RMS} \cdot \frac{4\,E_b}{E_b^2 - E_{b_o}^2}$$

TEST PROCEDURE

Since it was not possible to make all measurements instantaneously, a constant mean center-line velo ity at the outlet was maintained by keeping the flow rate constant, i.e., keeping the manometer reading constant for every run in each series of experiments.

Two series of experiments were undertaken; one using a single jet (Fig. 7), the other with multiple jets (Fig. 8). Five different conditions of outlet turbulence intensity (ϵ_o = 3, 6, 12, 25 and 40 per cent respectively) were established for each series while the outlet velocities were always kept at 515 fpm for the single jet and 1400 fpm for the multiple jets. The outlet velocities were so chosen that the main jet would just hit the opposite wall of the test chamber while using Titanium Tetra-Chloride ($TiCl_4$) smoke to observe the flow patterns.

Velocities and turbulence intensities were measured at each test point on the center-line of the jet and in the occupied space. The center line of the jet was found to be almost horizontal, but deflected slightly toward the ceiling by flow induced pressure difference which is called the Coanda effect. A terminal velocity was arbitrarily defined as the velocity at 7/8 of the test chamber length at the center line of the jet and was found to be 80 fpm. The location of the test points on the center-line of the jet were shown in Fig. 10. Figure 11 shows the plan and end views of the test points in the occupied space. The plane of measurement was 1/3 the height of the model measured from the floor. The points were located along the center-line and a line 3.0 inches from the front wall. The flow conditions were assumed to be symmetrical within the model.

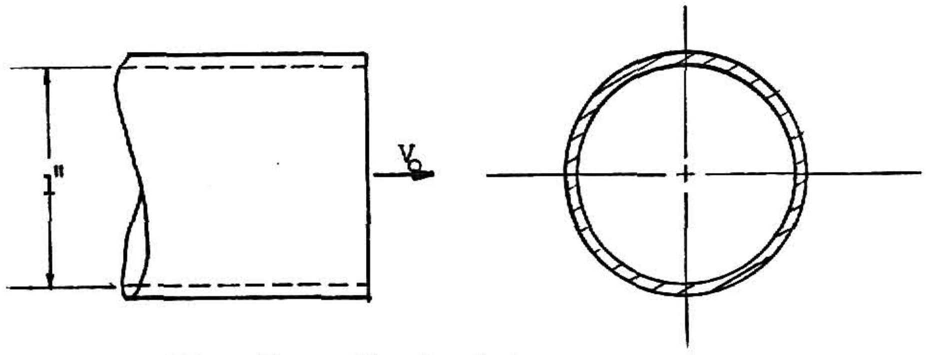

Fig. 7 Single Jet

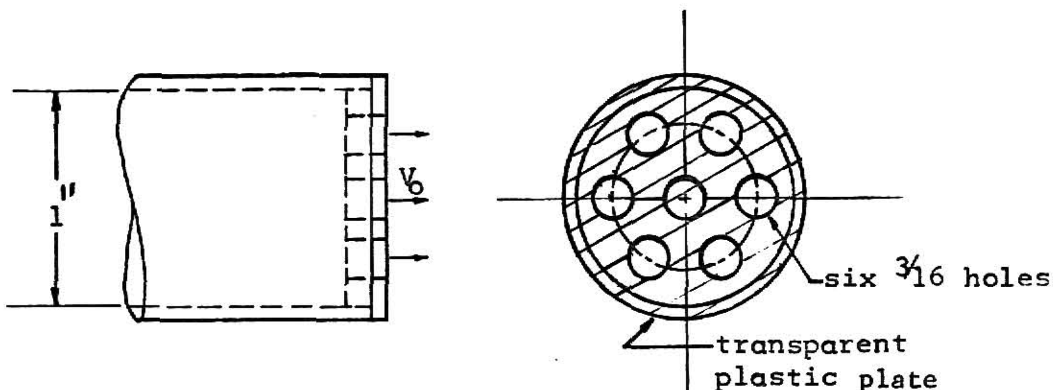

Fig. 8 Multiple Jets

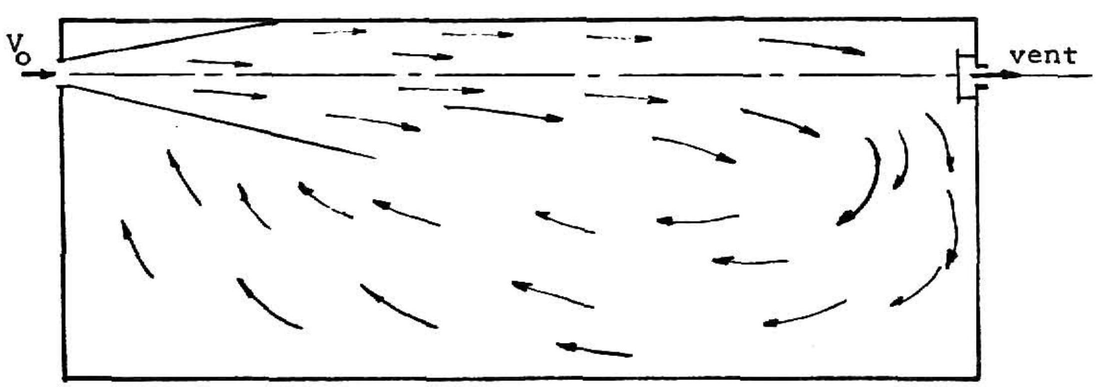

Fig. 9 General Air Distribution

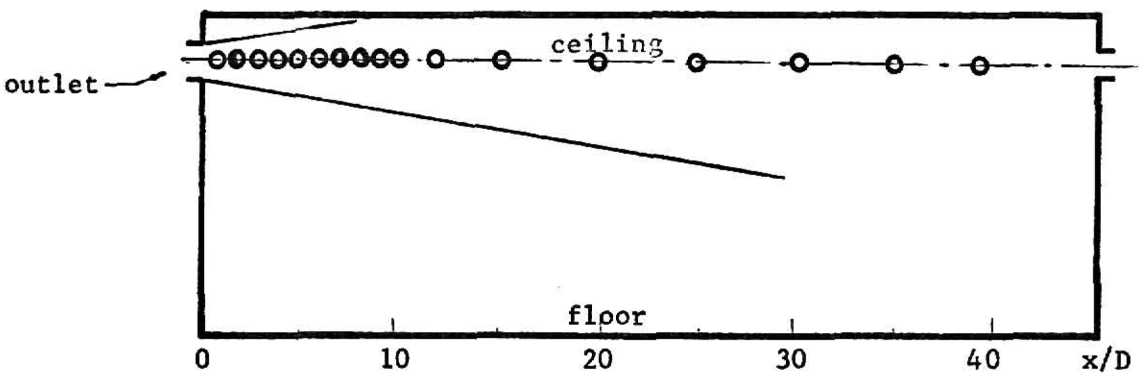

Fig. 10 Location og Test Points in Jet

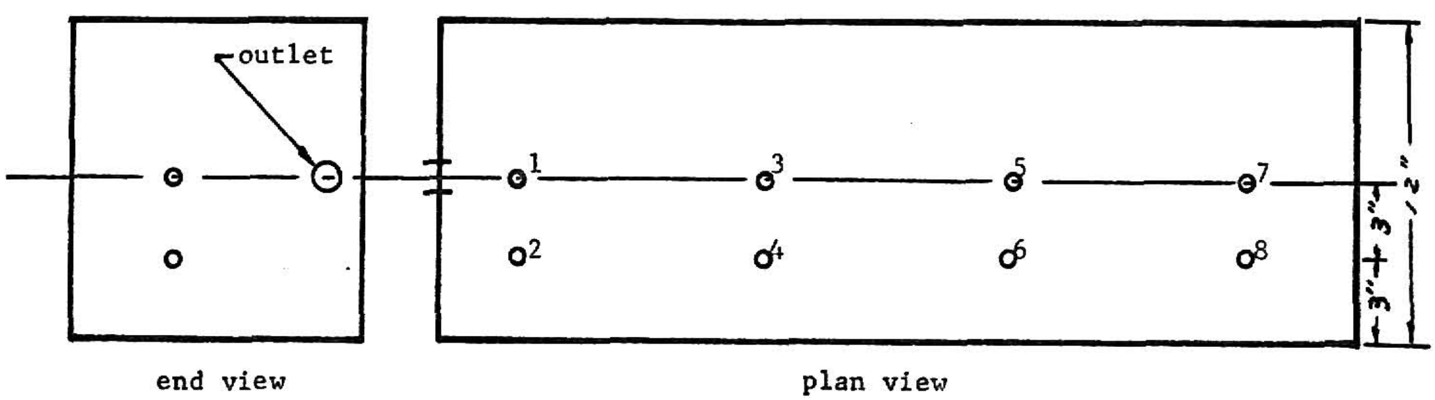

Fig. 11 Location of Test Points in the Occupied Space

For each test, the outlet conditions (velocity and turbulence intensity) were carefully established and allowed to stablize. The experimental conditions for both the 515 fpm single jet and 1400 fpm multiple jets are listed in tables I and II, respectively. The listed conditions are the different outlet turbulence intensities and their corresponding flow rates and temperatures. The jets were considered isothermal since the temperature differences between the outlet (T_o) and the exhaust (T_e) were no more than 0.4 F. Flow rates were computed by using Bernoulli's equation, nozzle coefficient, expansion factor, and the measured pressure difference across the 3/16 inch nozzle.

Measurements began 30 minutes after the test conditions had been set. The flow rate and the temperature at the outlet and exhaust were measured first. The hot-wire was placed horizontal and perpendicular to the air flow. While in the occupied space, the hot-wire was placed 45^o from the horizontal to obtain the best interaction between free and forced convection. The measured results were obtained from the arithmetic mean of ten values, recorded every ten seconds at each test point. It was found that the turbulence intensities were not steady in the occupied space, so that the ranges of the variations were observed over a period of two minutes. The 95% confidence interval was calculated for each point as shown in Figs. 22 to 37.

Table I. Experimental Conditions of the 515 fpm Single Jet

Outlet Turbulence Intensities	Flow Rate					Outlet Temp.	Exhaust Temp.
	Main	Jet	Total Flow		Estimated flow through the turbulence promotor		
ϵ_o, %	P^*, inches of water	cfm	P^*, inches of water	cfm	cfm	T_o, ^oF	T_e, ^oF
3.67	2.50	1.022	2.50	1.022	0.000	78.0	78.2
6.89	2.50	1.022	2.72	1.326	0.304	80.0	80.3
13.92	2.57	1.033	3.33	1.600	0.567	78.5	78.6
30.65	4.16	1.320	5.62	2.103	0.783	75.4	75.8
45.33	3.47	1.202	5.67	2.160	0.958	76.4	76.6

* pressure difference across a 3/16 inch nozzle

Table II. Experimental Conditions of the 1400 fpm Multiple Jets

Outlet Turbulence Intensities	Flow Rate					Outlet Temp.	Exhaust Temp.
	Main Jet		Total Flow		Estimated flow through the turbulence promotor		
ϵ_o, %	P^*, inches of water	cfm	P^*, inches of water	cfm	cfm	T_o, ^oF	T_e, ^oF
3.02	1.19	0.707	1.33	0.947	0.240	76.6	77.7
5.79	1.08	0.672	1.48	1.080	0.408	73.0	73.2
11.71	0.94	0.625	1.61	1.157	0.532	73.0	73.2
22.52	0.94	0.625	1.89	1.456	0.631	74.0	74.2
35.20	0.75	0.561	2.76	1.479	0.918	72.0	72.4

* pressure difference across a 3/16 inch nozzle

RESULTS AND DISCUSSION

The experimental results are shown in Figs. 13 to 39. For both single and multiple jets, Figs. 13 and 14 show how the turbulence intensities on the center-line in a jet vary in relation to the distance from the outlet as a function of outlet turbulence intensity. There was a sharp rise and then a drop in turbulence intensity for the low outlet turbulence level, but a sharp drop for the higher outlet turbulence level along the jet axis within a very short distance from the outlet. In general, the turbulence intensity apparently rises to some maximum value prior to an x/D of 15, then it decreases gradually. Significantly, the observed values of turbulence intensity approached essentially the same value at the terminal of the jet.

For the 515 fpm single jet, a significant effect was found as shown in Fig. 15. This shows that the outlet turbulence intensity has an important effect on the center-line velocity of the jet. An increase in outlet turbulence intensity decreased the throw of the jet as shown in Fig. 17. No appreciable change in center-line velocity variation or throw was found for the 1400 fpm multiple jets (Figs. 16 and 17). These results agree with a previous paper[2] in which it was suggested that the effect of turbulence would be appreciable only at outlet velocities of roughly 1000 fpm and below.

The effect of outlet turbulence intensity upon velocities in the occupied space appears to be random and inconclusive as shown in Figs. 18 to 21. The effect of outlet turbulence intensity upon turbulence intensities in the occupied space is shown in Figs. 22 to 37. In addition to the range of measurement, the 95% confidence interval is given. However, considering the uncertainty of the measurements in the occupied space, which was about ±5 fpm for velocities and ±5% for turbulence intensities (see appendix for details), the effects shown in Figs. 18 to 37 were almost all within the range of the uncertainties, thus probably the effect is nil. Another approach was applied to the analysis to these random type results. The average velocities and turbulence intensities were obtained by taking the arithmetic mean of 12 points in the occupies space as shown in Fig. 12 where the data for points 9, 10, 11 and 12 were assumed as the same as that of points 2,4,6 and 8 respectively.

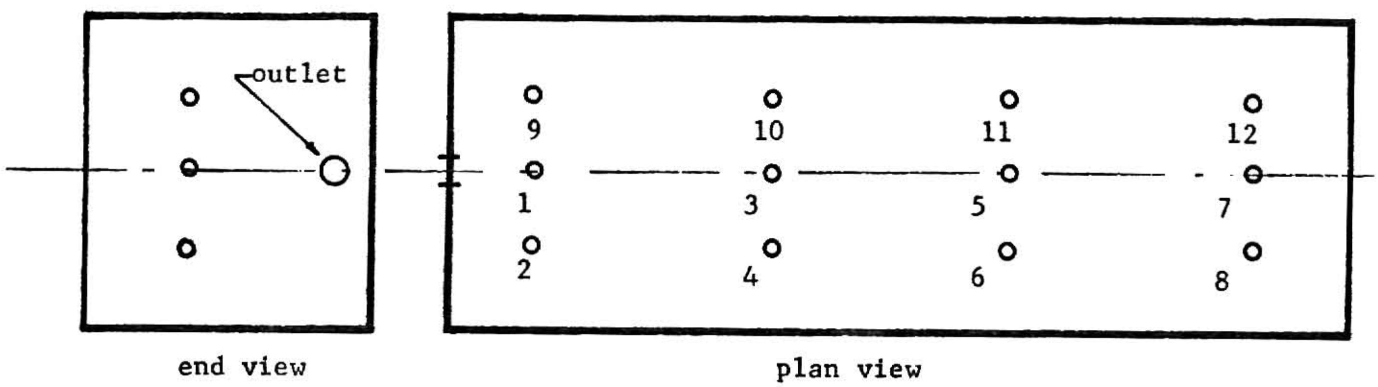

Fig. 12 Test Points for the Average Values in the Occupied Space

The data shown in Fig. 38 indicated that the average velocities in the occupied space tended to increase with increasing outlet turbulence intensities. With consideration of the uncertainty of the velocity measurement, this can only be considered to be a trend, statistically the effect is nil. The average turbulence levels in the occupied zone are shown in Fig. 39. The differences are not significant especially for those outlet turbulence intensities less than 20%.

In all cases, an increase in air flow rate was required to generate the higher outlet turbulence intensities. The following is an attempt to explain the effect of the outlet turbulence intensity on the averaged velocity and turbulence level in the occupied space.

From the view-point of a momentum analysis, Figs. 40 and 41 show the effect of outlet momentum rates on the average velocity and average turbulence level in the occupied space. The momentum in the outlet center was calculated by the equation

$$M_o = \rho\, Q_t \frac{Q_t}{A_o} = \rho \cdot \frac{Q_t^2}{A_o}$$

where M_o = momentum rate at the outlet, lb_f

ρ = density of air, lb_m/ft^3

Q_t = total flow rate, ft^3/sec

A_o = gross outlet area, ft^2

Considering Figs. 38 and 39 and Figs. 40 and 41, it appears that outlet turbulence intensity and outlet momentum rate may have similar effect on the average velocity and turbulence level in the occupied space. It is noted that the main flow rates for the tests with the 1400 fpm multiple jets were much less than those for the 515 fpm single jet, but the estimated percentage of flow added due to the turbulence promotor of the former were much greater than those of the latter as shown in Fig. 42. This implies that added radially inward flow increases both the outlet turbulence intensity and outlet momentum rate and probably the average velocity in the occupied space as might be expected.

From the view-point of a statistical analysis, a two-way analysis of variance, with 5% risk and test-points blocked, was used to detect statistically the effect of outlet turbulence intensity upon the turbulence level in the occupied space. The results of the analysis were shown in Tables III to VIII. The interaction effect of the outlet turbulence level and the location in the occupied space were significant for both the 515 fpm single jet and the 1400 fpm multiple jets as shown in Tables III and VI. From Tables V and VIII, the "Least Significant Difference" (LSD) was tested for each point in the occupied space, the values with the same underline denote no significant difference within 95% confidence limits. This indicates that for an outlet turbulence intensity less than 20%, there is no significant effect on the turbulence level in the occupied space. For the outlet turbulence intensities above 20%, the effects are still small and not significant for engineering use.

THIS BOOK CONTAINS NUMEROUS PAGES THAT WERE BOUND WITHOUT PAGE NUMBERS.

THIS IS AS RECEIVED FROM CUSTOMER.

EXPLANATION OF TABLES III TO VIII

Two-way analysis of variance with 5% risk to detect the effects of outlet turbulence intensity upon the turbulence intensity in the occupied space.

For the 515 fpm single jet (Plate III),

$$LSD_{0.05} = t_{0.025,(DF_{err})} \cdot \sqrt{MS_{err} \cdot \frac{2}{n}}$$

$$= 1.96 \; (1.83)$$

$$= 3.587$$

For the 1400 fpm multiple jets (Plate IV),

$$LSD_{0.05} = 1.96 \; (1.966)$$

$$= 3.855$$

Table III Analysis of Variance Table for the 515 fpm Single Jet

Source of Variation	Degrees of Freedom	sum of Squares	Mean Square	F
Treatments (ϵ_o)	4	2872.06	718.0	43.1
Blocks (pt.)	7	8165.56	1167.0	69.9
Interaction (ϵ_o x pt.)	28	9499.94	339.0	20.8
Error	369	6167.56	16.7	
Total	399	26705.13		

Table IV Turbulence Intensities in the Occupied Space

ϵ_o \ pt.	1	2	3	4	5	6	7	8	$\overline{X}_{i..}$
1	16.77*	18.06	20.64	18.68	23.54	27.50	25.85	22.22	21.66
2	21.83	21.03	17.12	19.96	20.47	18.63	25.68	17.11	20.23
3	10.14	14.14	20.74	16.88	22.27	19.53	24.62	16.48	18.40
4	22.79	16.51	21.46	18 [illegible]1	26.49	28.45	26.07	41.03	25.27
5	6.98	8.86	18.62	25.50	27.70	34.31	32.28	42.17	24.55
$\overline{X}_{.j.}$	15.70	15.80	19.71	20.00	24.09	25.68	26.90	27.80	$\overline{X}_{...}$ = 21.96

*data in each experimental unit is the mean value of 10 observations

Table V LSD Test within Location for Different ϵ_o

pt. 1 ϵ_o : 4 2 1 3 5	pt. 2 ϵ_o : 2 1 4 3 5
pt. 3 ϵ_o : 4 3 1 5 2	pt. 4 ϵ_o : 5 2 4 1 3
pt. 5 ϵ_o : 5 4 1 3 2	pt. 6 ϵ_o : 5 4 1 3 2
pt. 7 ϵ_o : 5 4 1 2 3	pt. 8 ϵ_o : 5 4 1 2 3

Table VI Analysis of Variance Table for the 1400 fpm Multiple Jets

Source of Variation	Degrees of Freedom	Sum of Squares	Mean Square	F
Treatments (ϵ_o)	4	4419.06	1105.0	57.8
Blocks (pt.)	7	21445.94	3065.0	160.4
Interaction (ϵ_o x pt.)	28	3927.06	140.0	7.3
Error	369	7064.13	19.1	
Total	399	36856.19		

Table VII Turbulence Intensities in the Occupied Space

ϵ_o \ pt.	1	2	3	4	5	6	7	8	$\overline{X}_{i..}$
1	18.06*	14.62	23.52	25.30	26.44	29.37	33.23	34.44	25.63
2	19.06	12.56	7.24	26.30	26.10	22.94	32.51	31.71	22.30
3	17.60	18.29	24.00	21.15	25.58	30.85	35.42	36.28	26.15
4	24.43	17.47	23.11	21.58	32.60	27.42	43.55	36.88	28.38
5	21.69	18.29	29.13	33.74	29.13	33.76	44.10	48.77	32.33
$\overline{X}_{.j.}$	20.17	16.25	21.40	25.61	27.97	28.87	37.76	37.61	$\overline{X}_{...}$ = 26.96

*data in each experimental unit is the mean of 10 observations

Table VIII LSD Test within Location for Different ϵ_o

pt. 1	ϵ_o :	4	5	2	1	3	pt. 2	ϵ_o :	5	3	4	1	2
pt. 3	ϵ_o :	5	3	1	4	2	pt. 4	ϵ_o :	5	2	1	4	3
pt. 5	ϵ_o :	4	5	1	2	3	pt. 6	ϵ_o :	5	3	1	4	2
pt. 7	ϵ_o :	5	4	3	1	2	pt. 8	ϵ_o :	5	4	3	1	2

CONCLUSIONS

The results obtained from this research are summarized as follows:

1. The center-line turbulence intensity in a jet reaches a maximum value prior to an x/D of 15, then decreases gradually and approaches a level at the termination of the jet which appears to be independent of turbulence intensity at the outlet.

2. The jet throw was decreased apparently by higher outlet turbulence level for the single jet, but no appreciable change with outlet turbulence level was observed for the multiple jets.

3. The turbulence intensity at any given point in the occupied space was random and unsteady.

4. The added flow rate for the turbulence promoter probably increased the air velocities in the occupied space (due to the increased outlet momentum rate) and masked the effect of increased outlet turbulence intensity.

5. For outlet turbulence intensities less than 20%, no significant effect was found upon the turbulence level in the occupied space.

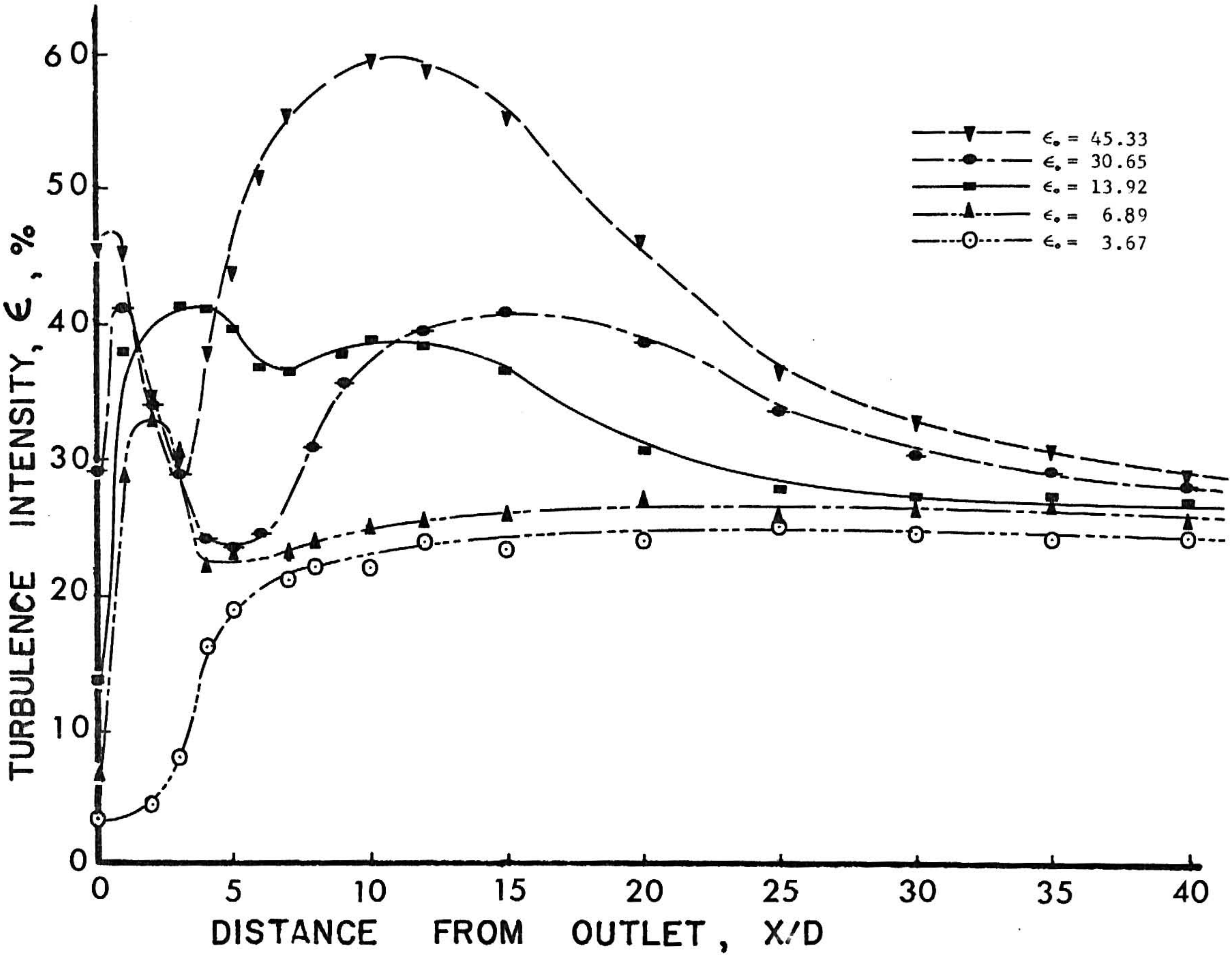

Fig. 13 Distribution of the Center-line Turbulence Intensity of the 515 fpm Single Jet

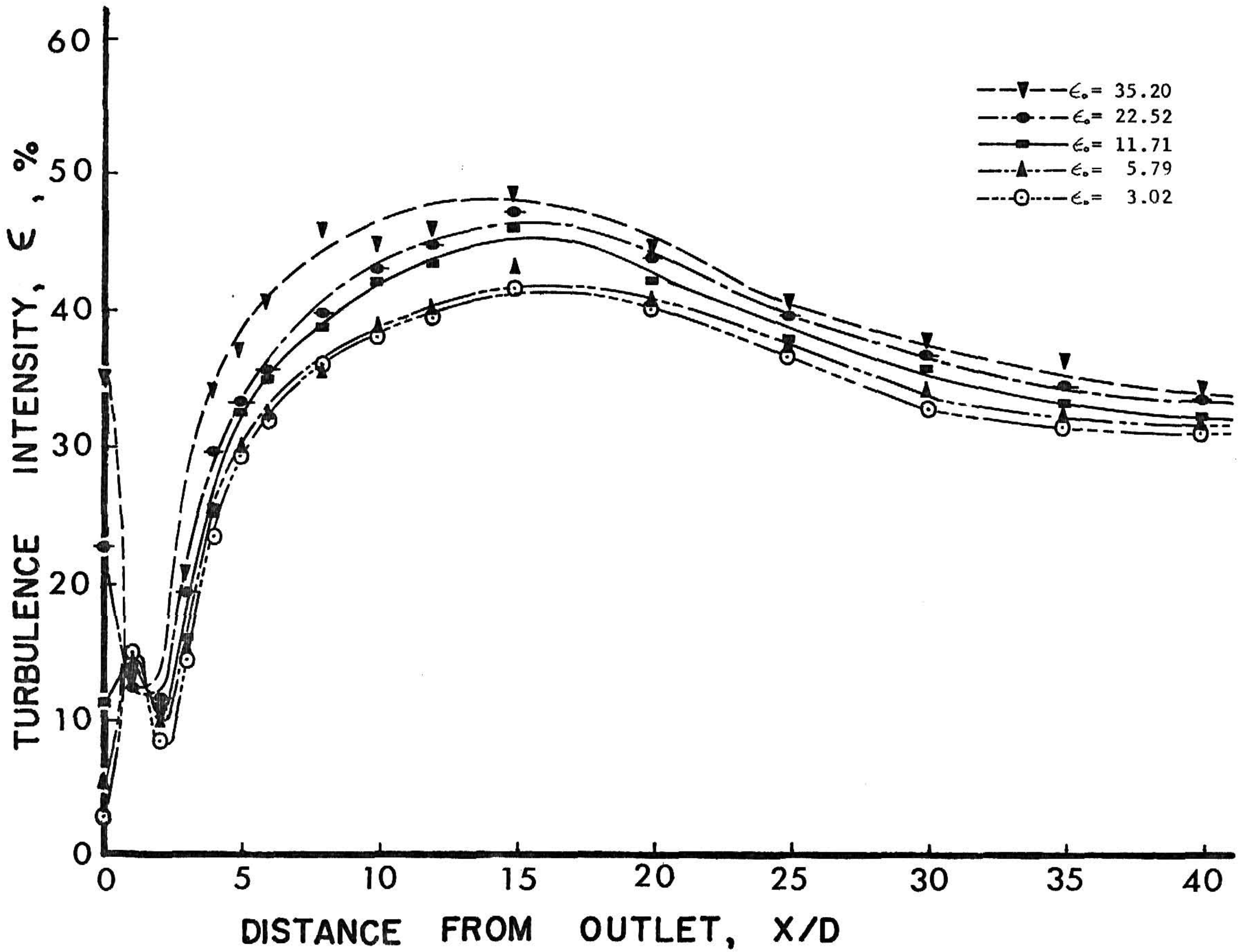

Fig. 14 Distribution of the Center-line Turbulence Intensity of the 1400 fpm Multiple Jets

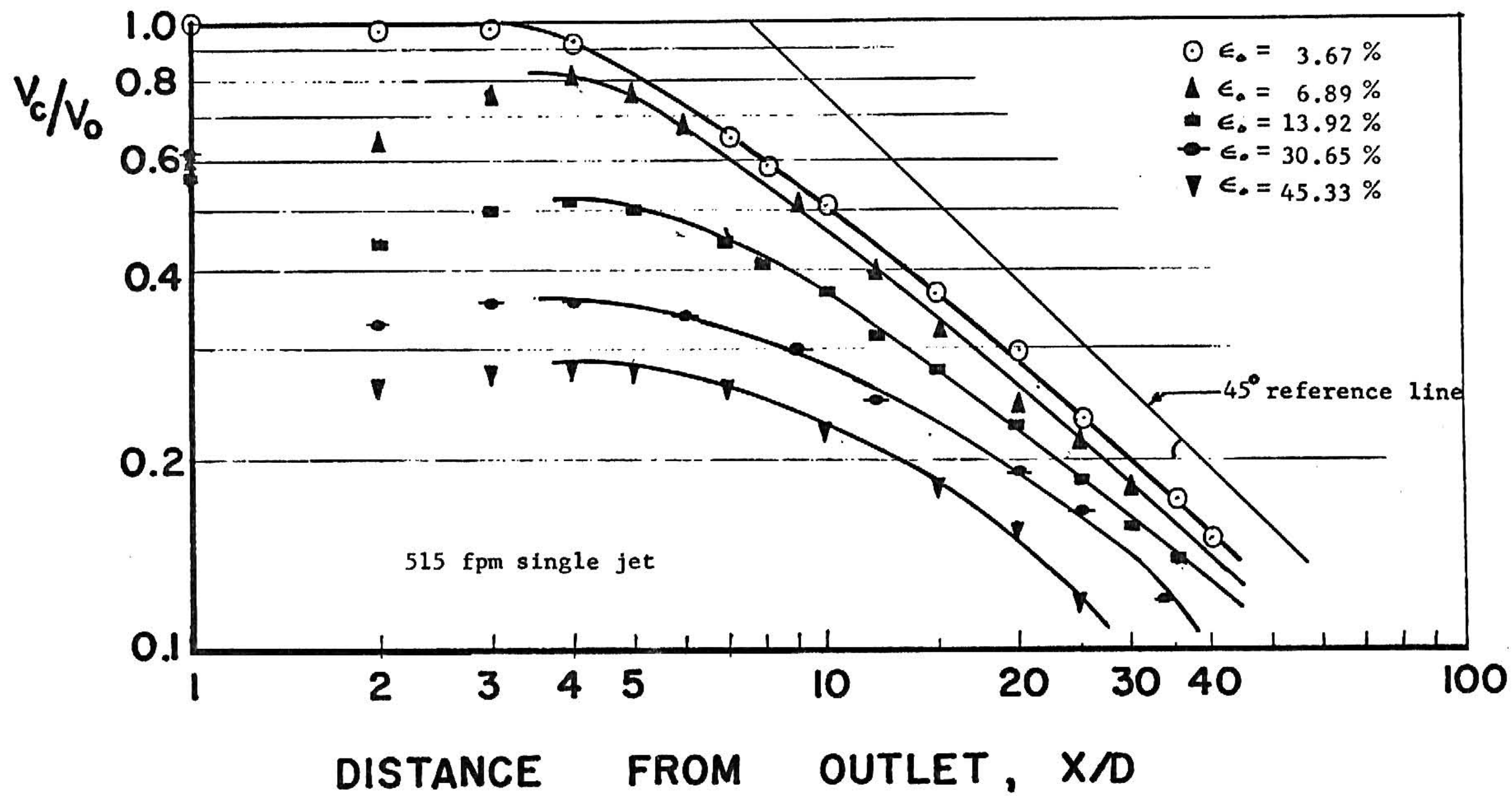

Fig. 15 Distribution of the Center-line Velocity for Different Outlet Turbulence Intensities

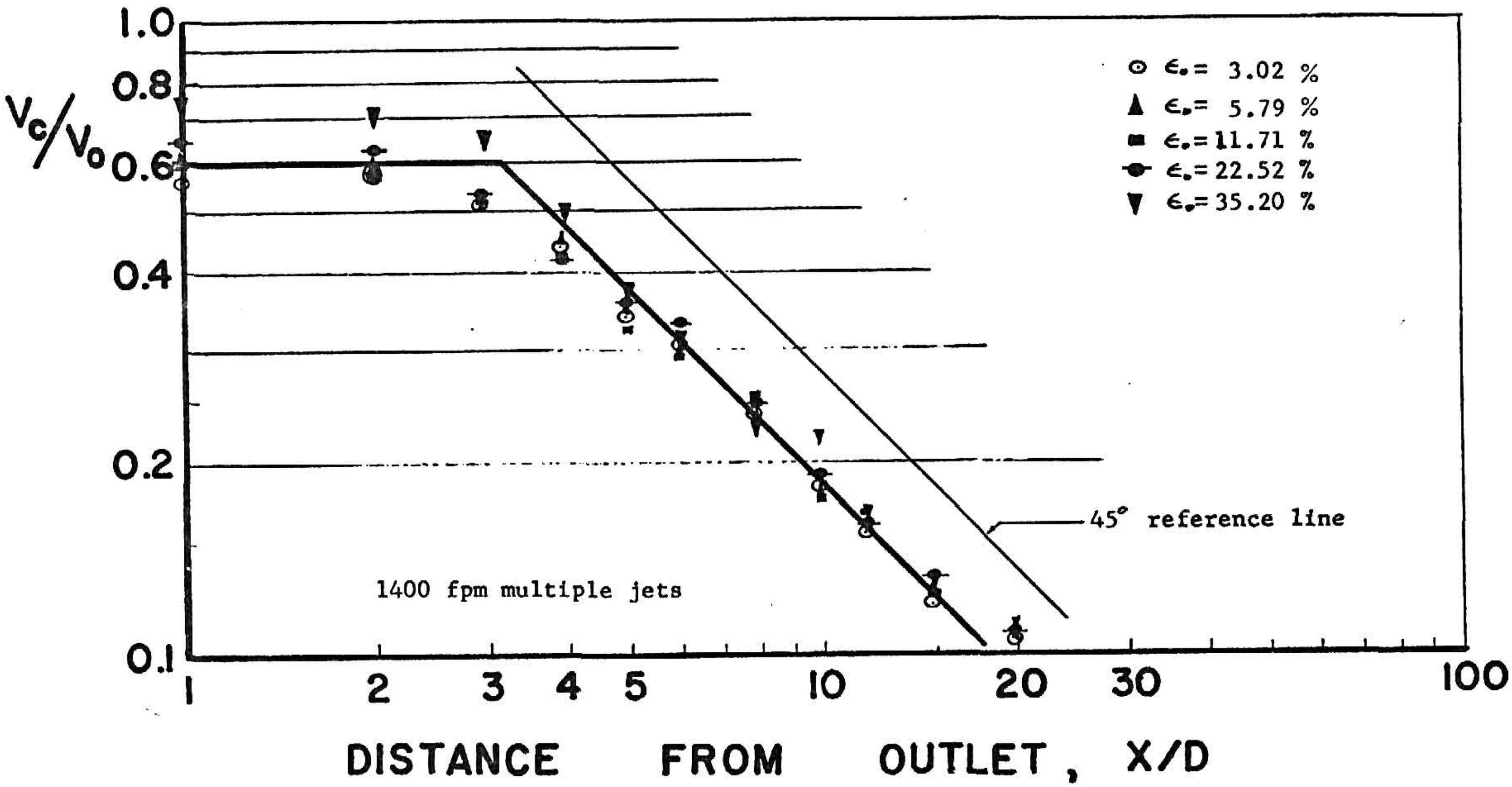

Fig. 16 · Distribution of the Center-line Velocity for Different Outlet Turbulence Intensities

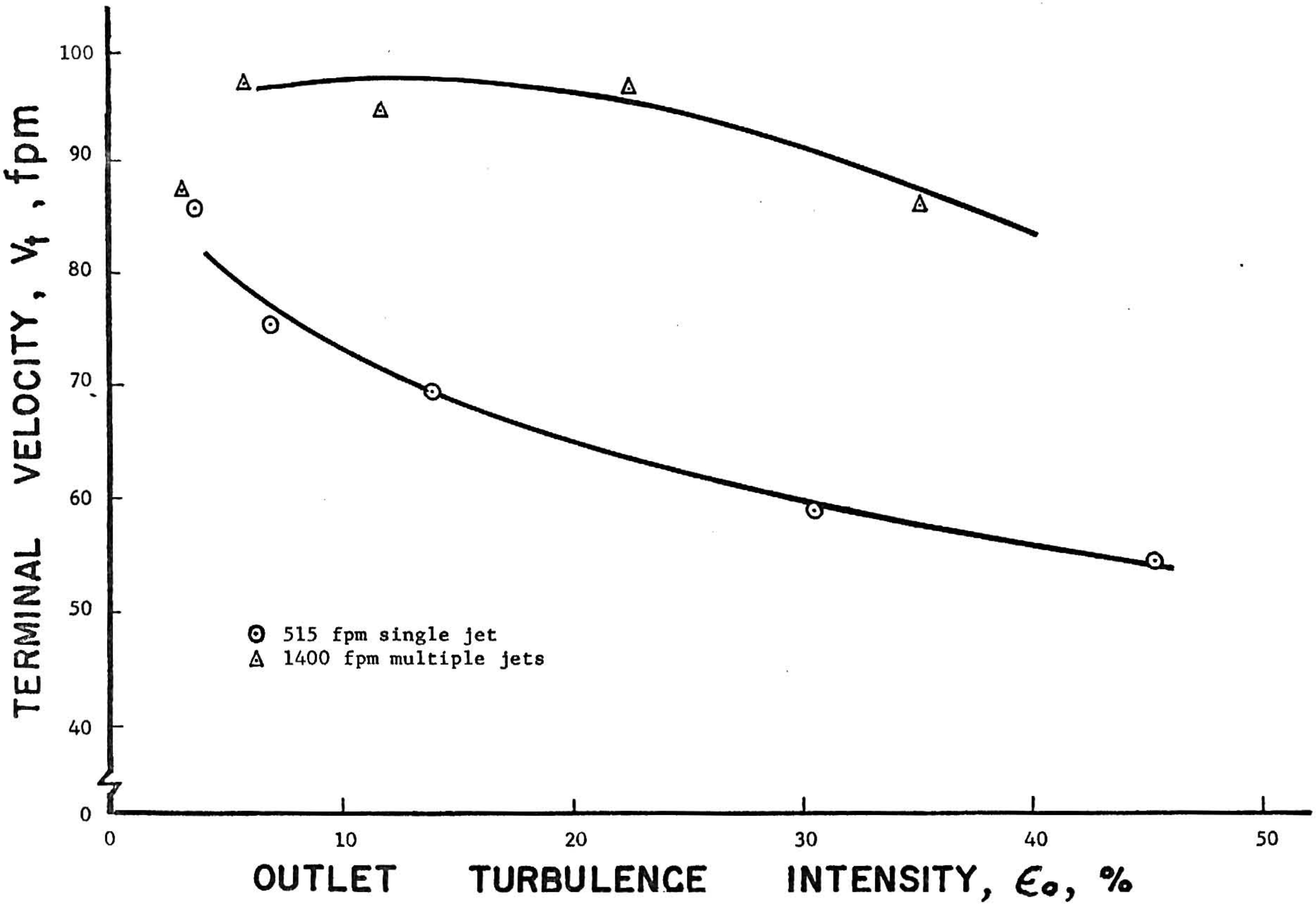

Fig. 17 Variation of Terminal Velocities (Throws) Resulting from Different ϵ_o

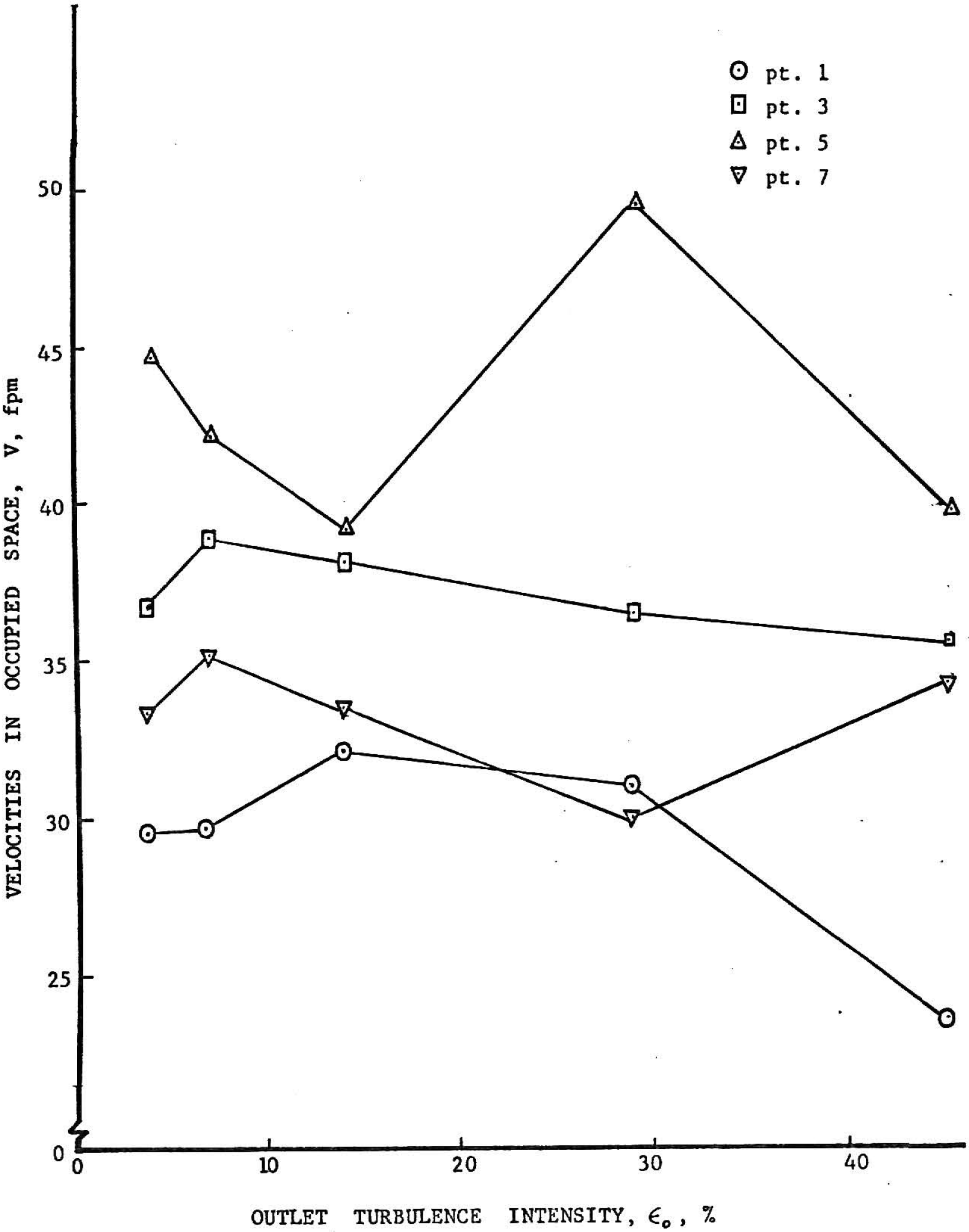

Fig. 18 Velocity Variations in the Occupied Space of the 515 fpm Single Jet for Different Outlet Turbulence Intensities (Points Located at the Center-line of the Chamber)

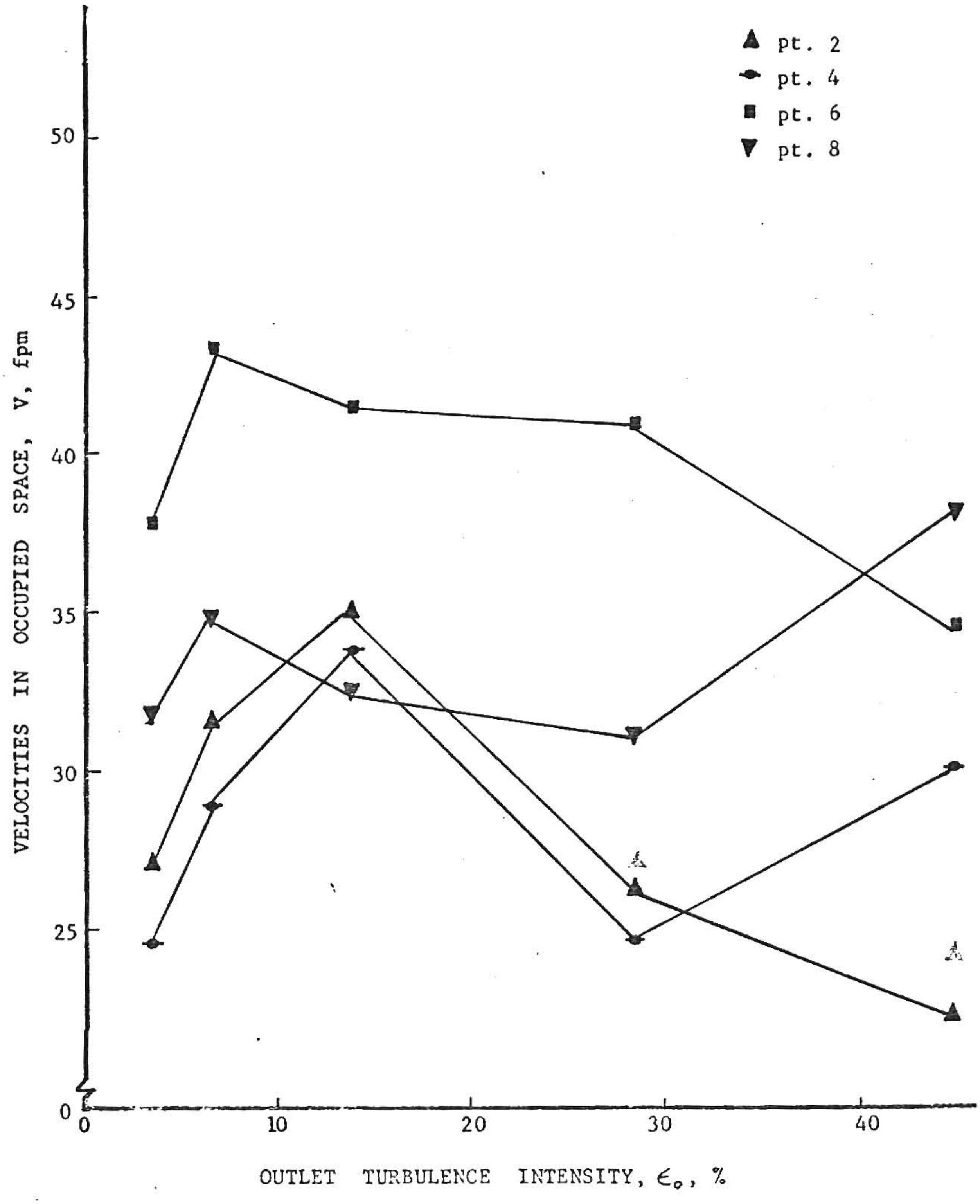

Fig. 19 Velocity Variations in the Occupied Space of the 515 fpm Single Jet for Different Outlet Turbulence Intensities (Points Located at Half Side of the Chamber)

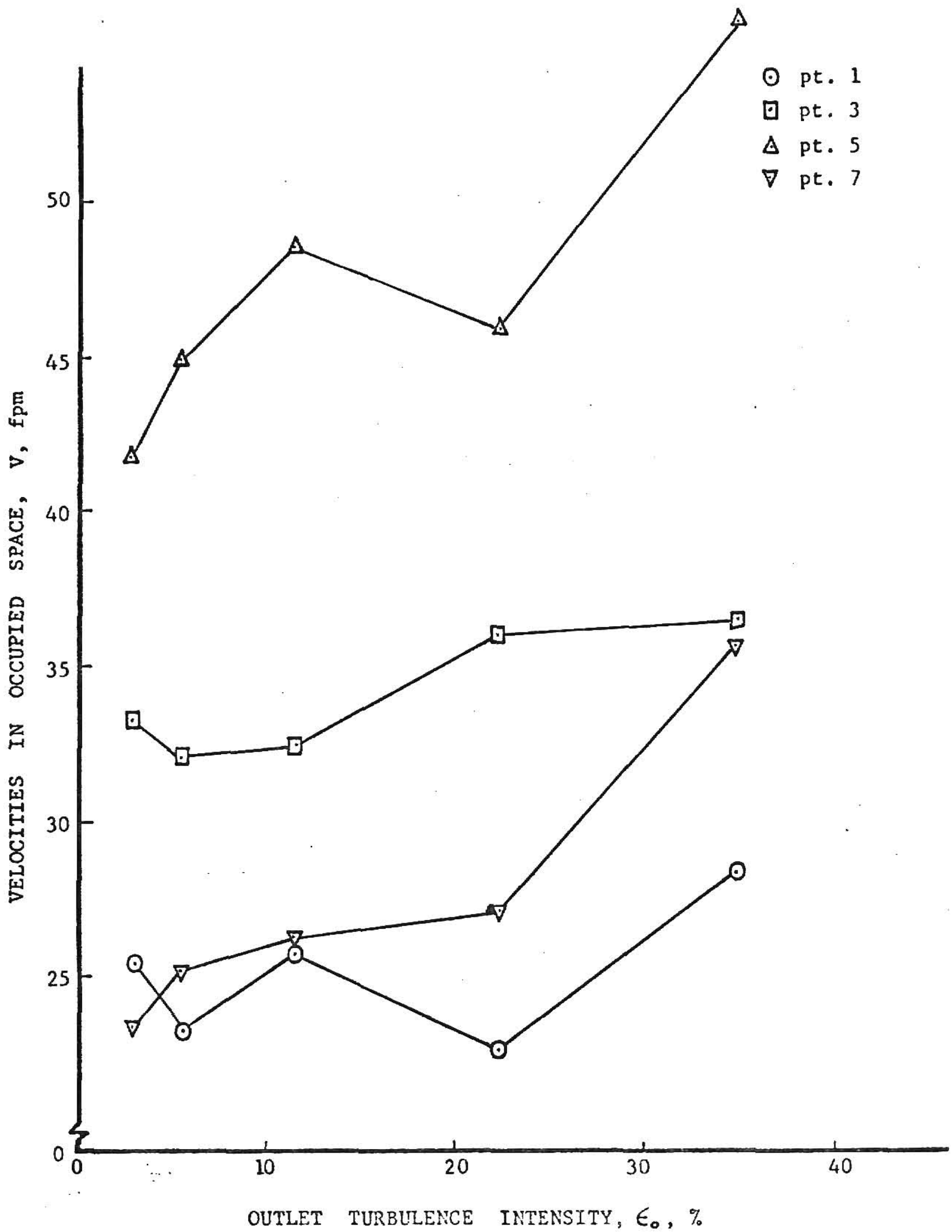

Fig. 20 Velocity Variations in the Occupied Space of the 1400 fpm Multiple Jets for Different Outlet Turbulence Intensities (Points Located at the Center-line of the Chamber)

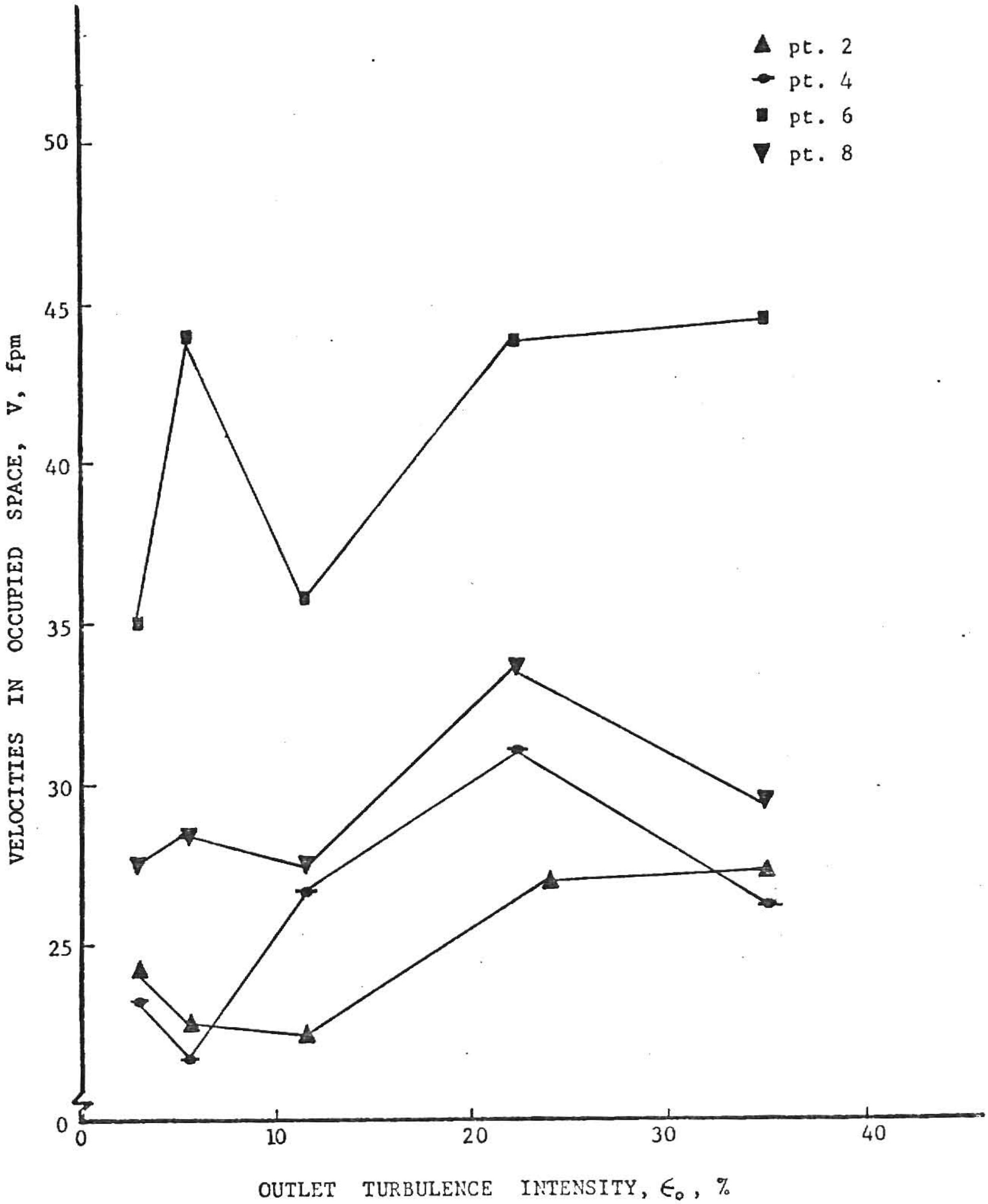

Fig. 21 Velocity Variations in the Occupied Space of the 1400 fpm Multiple Jets for Different Outlet Turbulence Intensities (Points Located at Half Side of the Chamber)

EXPLANATION OF FIGURES 22 TO 29

Variations of turbulence intensity, mean value and 95% confidence interval in the occupied space for a 515 fpm single jet for different turbulence intensities. Location of the test points were shown in Fig. 11.

represents the 95% confidence interval

represents the variation range

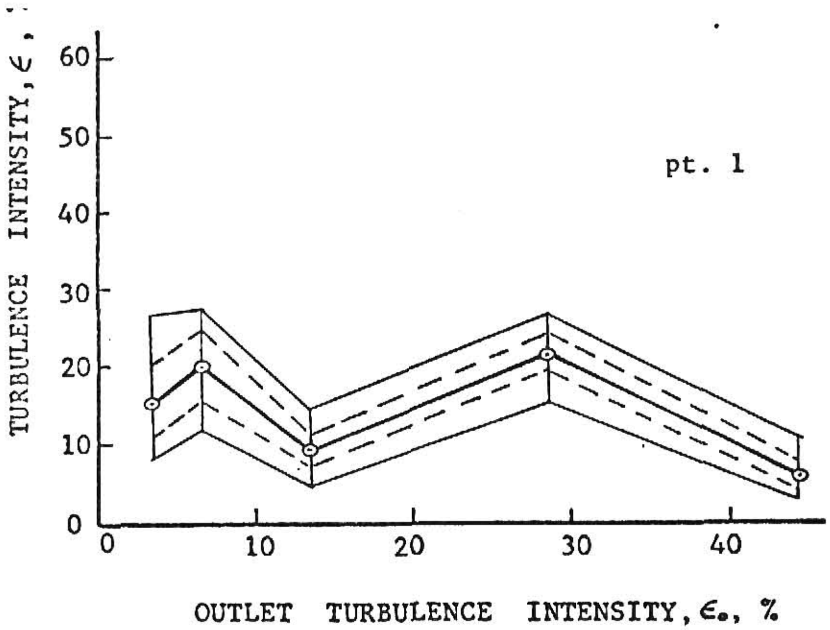

Fig. 22

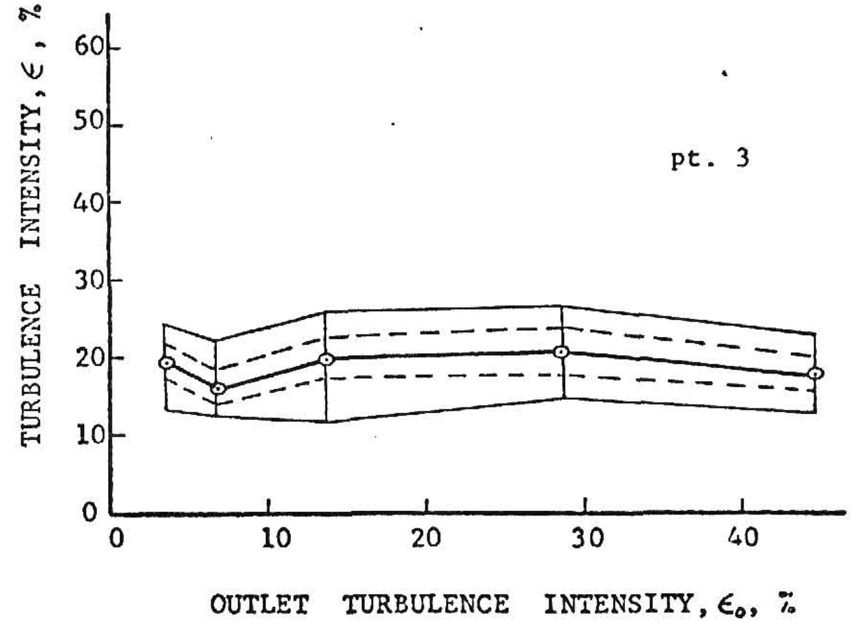

Fig. 23

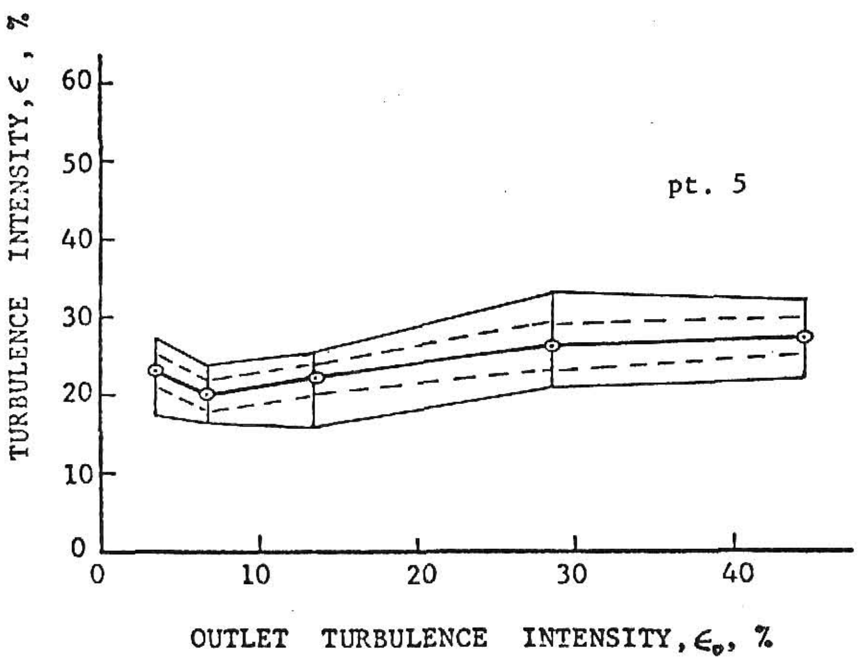

Fig. 24

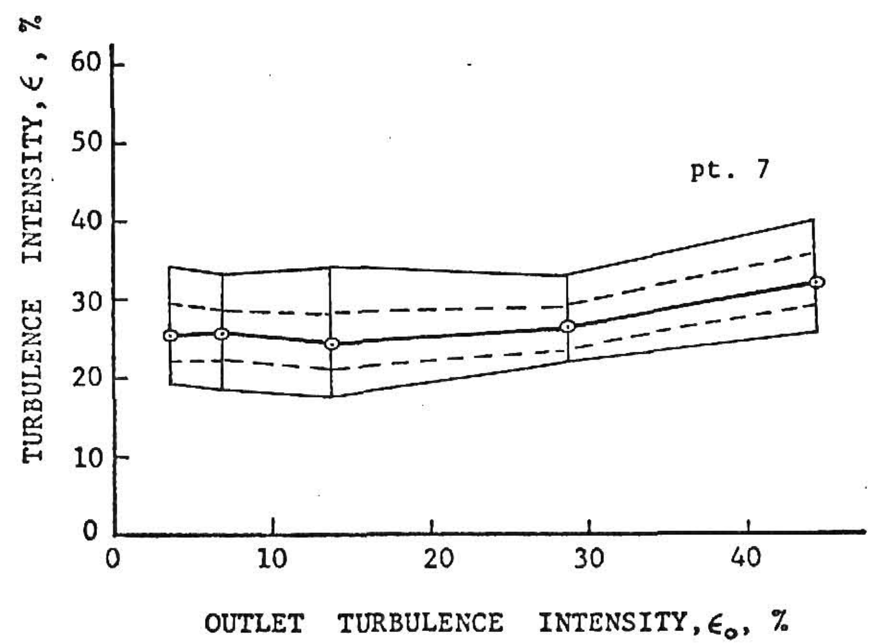

Fig. 25

ILLEGIBLE

THE FOLLOWING DOCUMENT (S) IS ILLEGIBLE DUE TO THE PRINTING ON THE ORIGINAL BEING CUT OFF

ILLEGIBLE

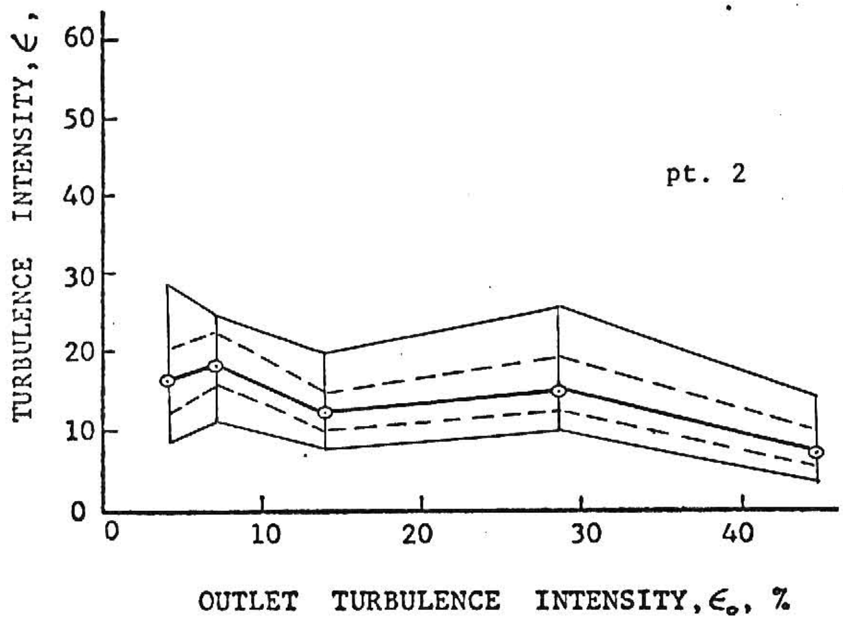

Fig. 26

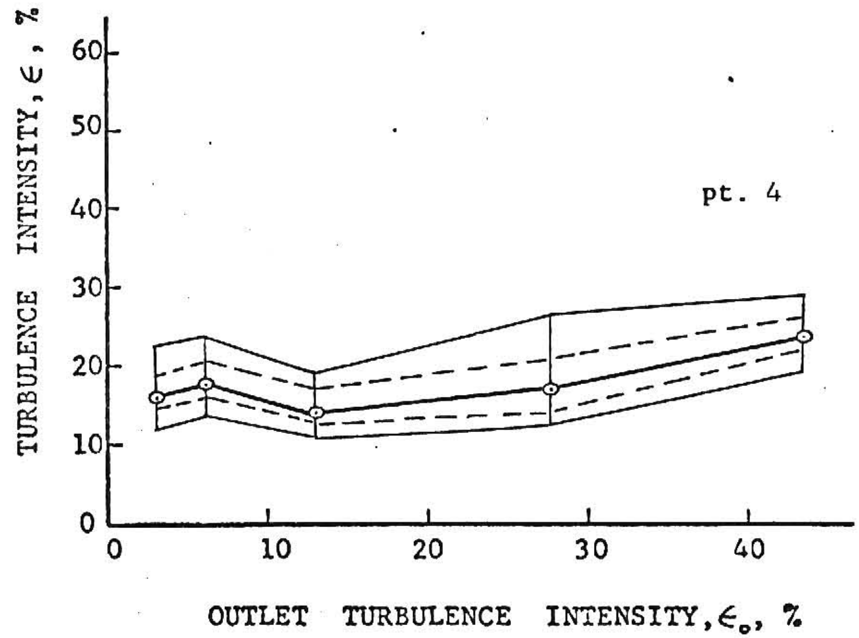

Fig. 27

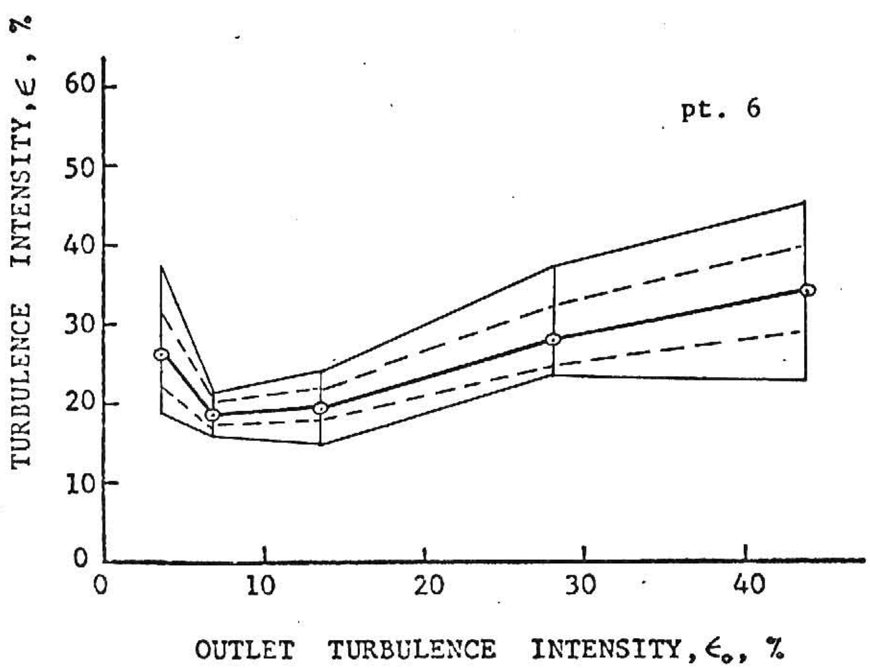

Fig. 28

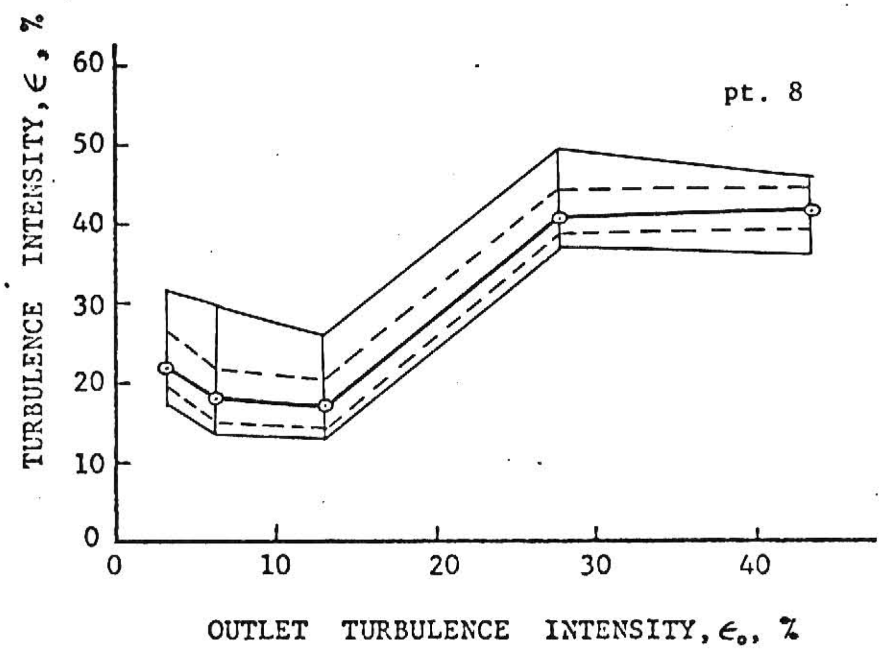

Fig. 29

EXPLANATION OF FIGURES 30 TO 37

Variations of turbulence intensity, mean value and 95% confidence interval in the occupied space for a 1400 fpm multiple jets for different outlet turbulence intensities. Location of the test points were shown in Fig. 11.

 represents the 95% confidence interval

 represents the variation range

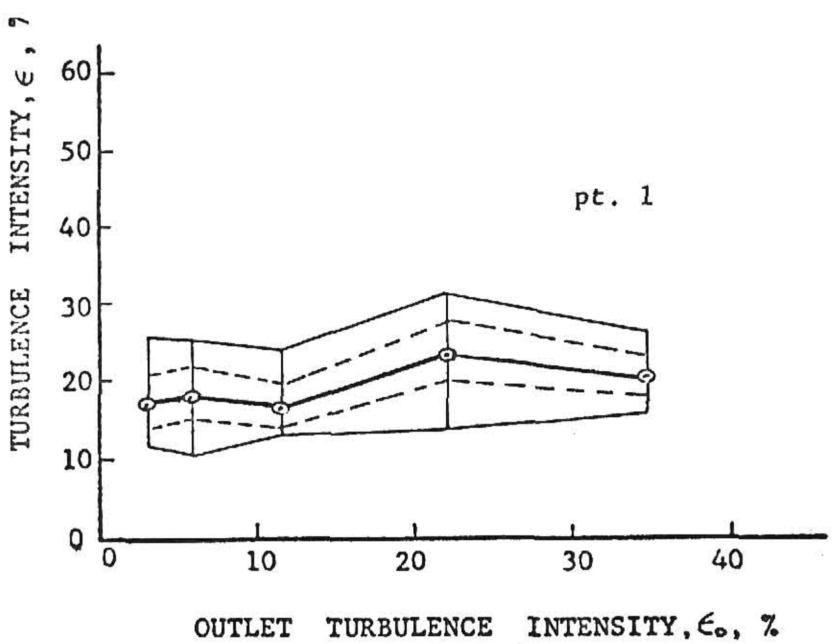

Fig. 30

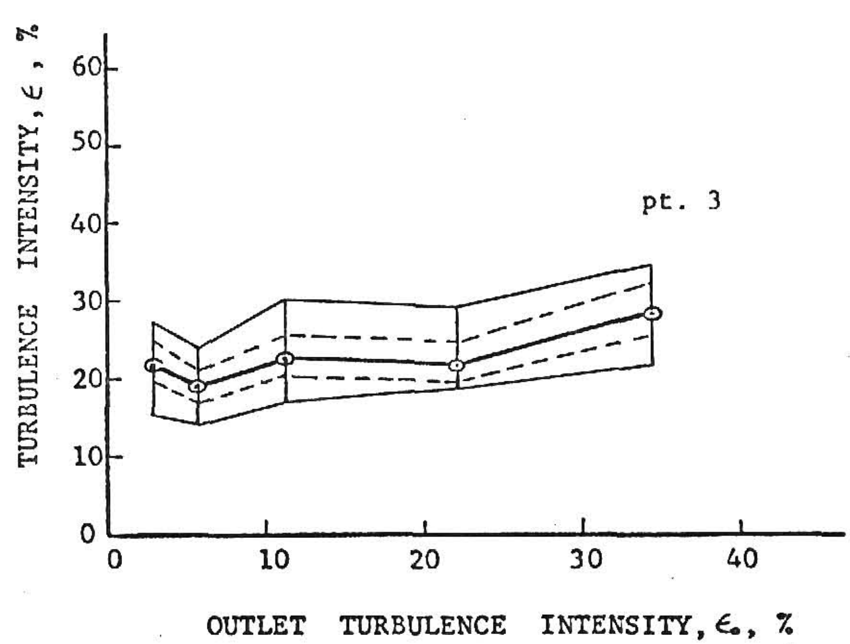

Fig. 31

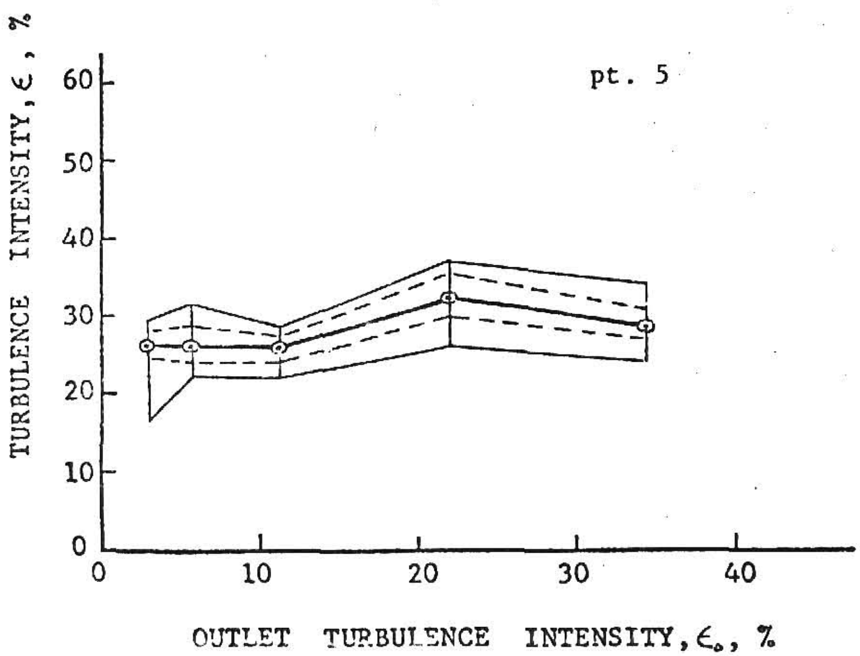

Fig. 32

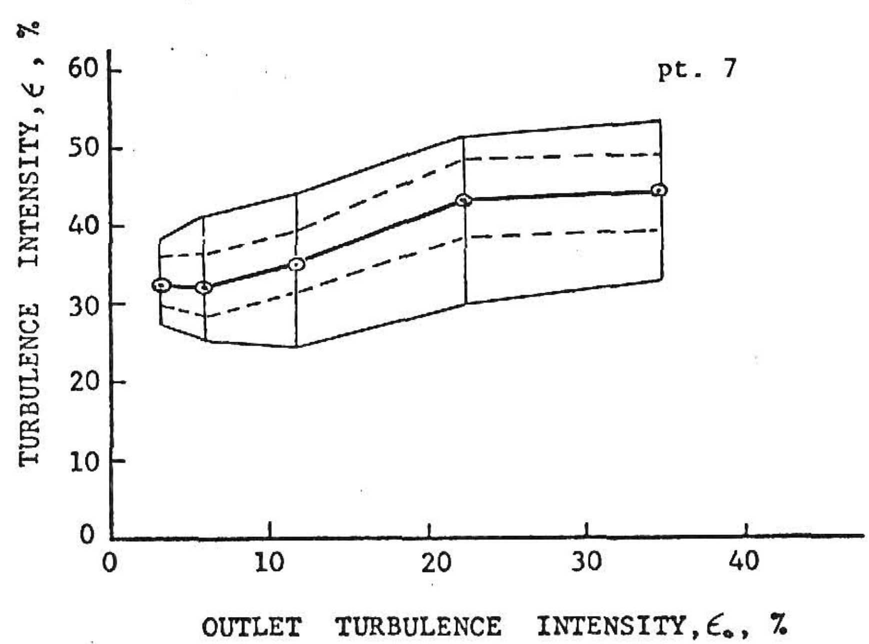

Fig. 33

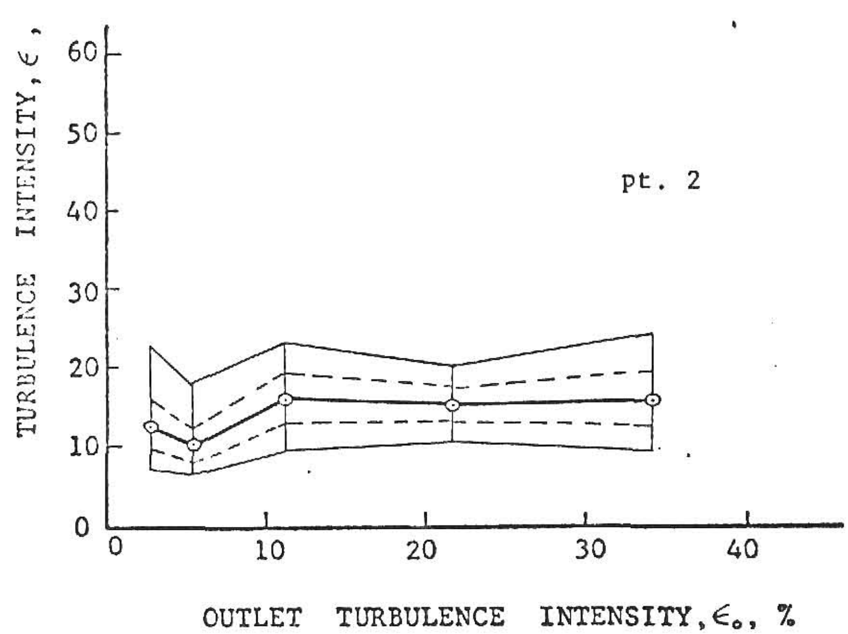

Fig. 34

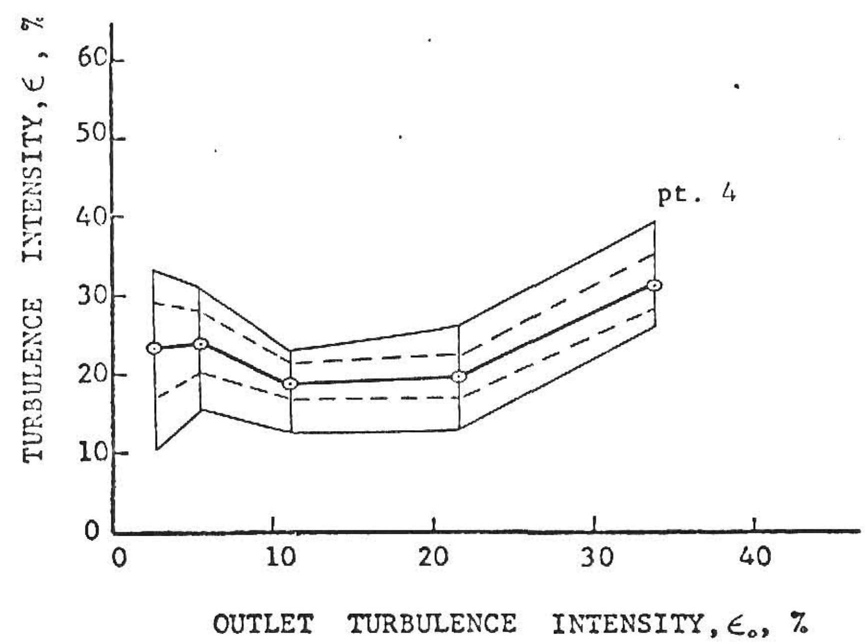

Fig. 35

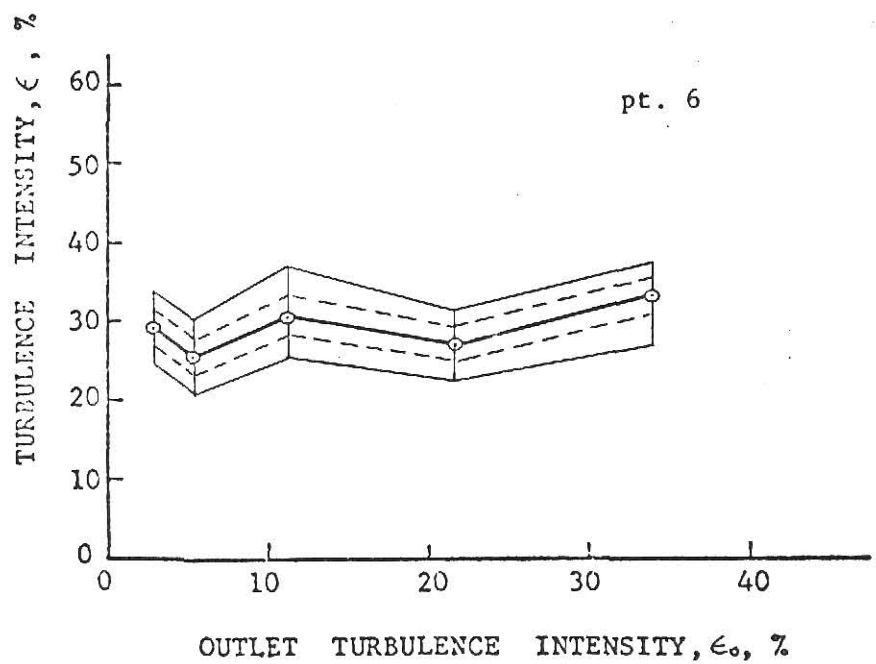

Fig. 36

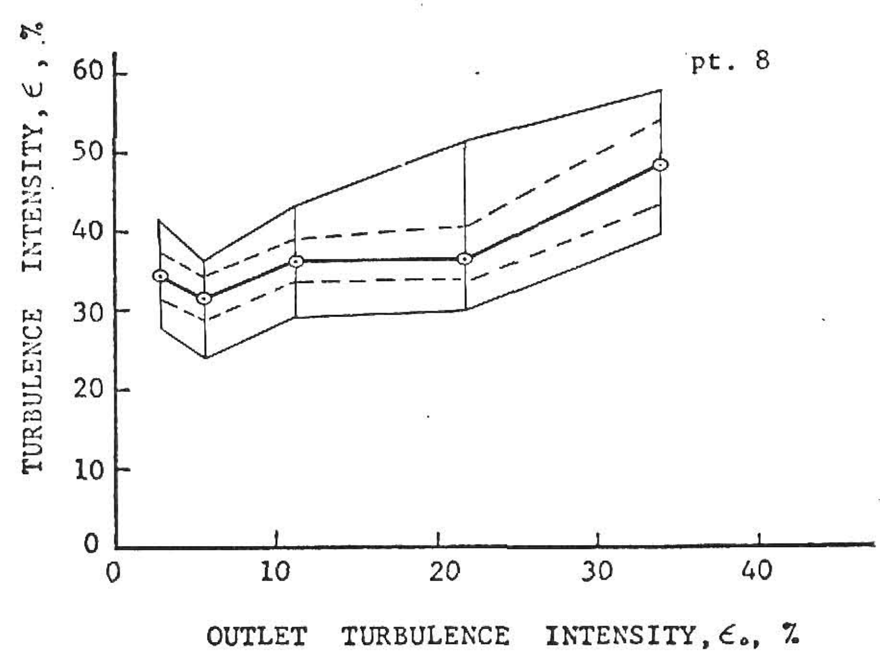

Fig. 37

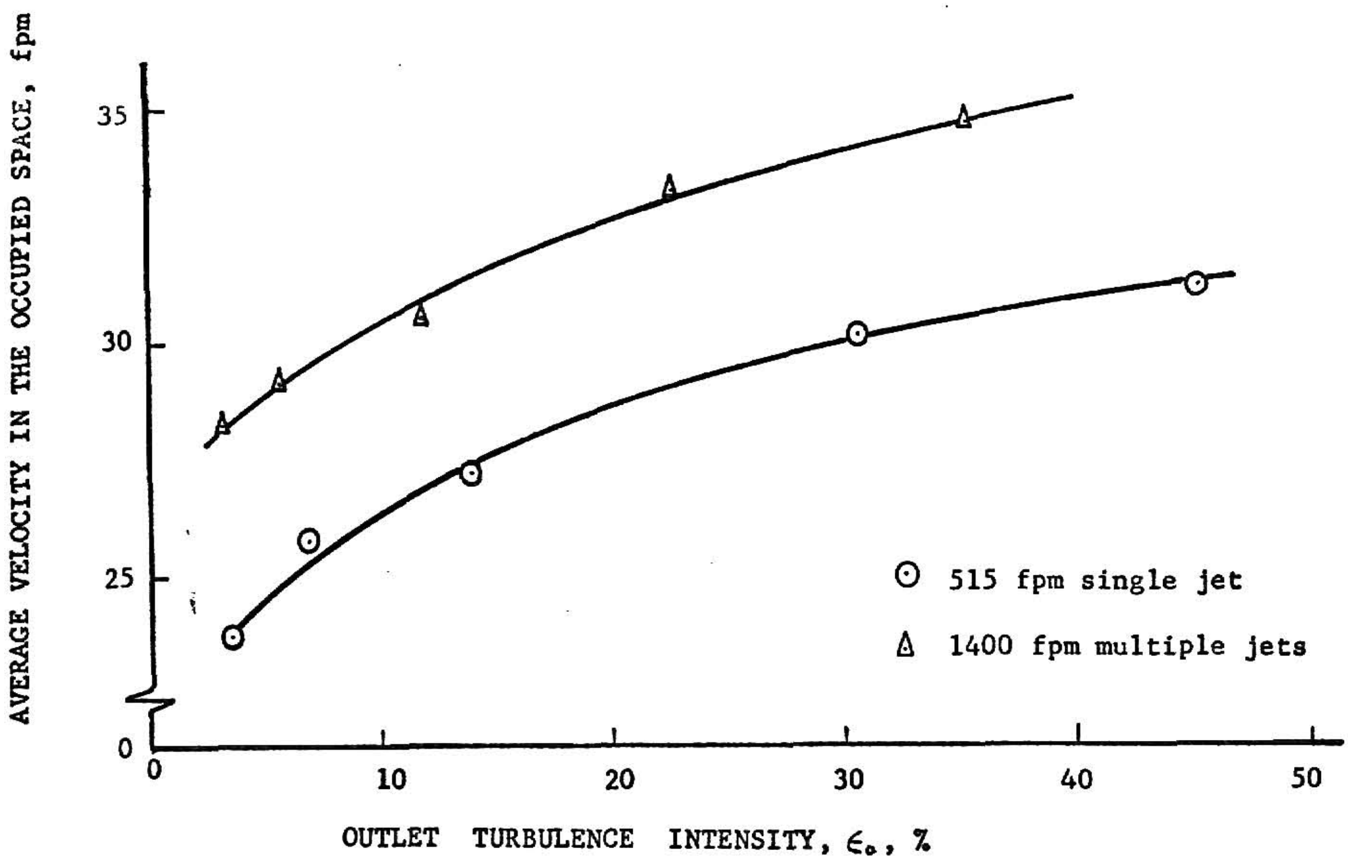

Fig. 38 Average Velocity Variations in the Occupied Space for Different Outlet Turbulence Intensities

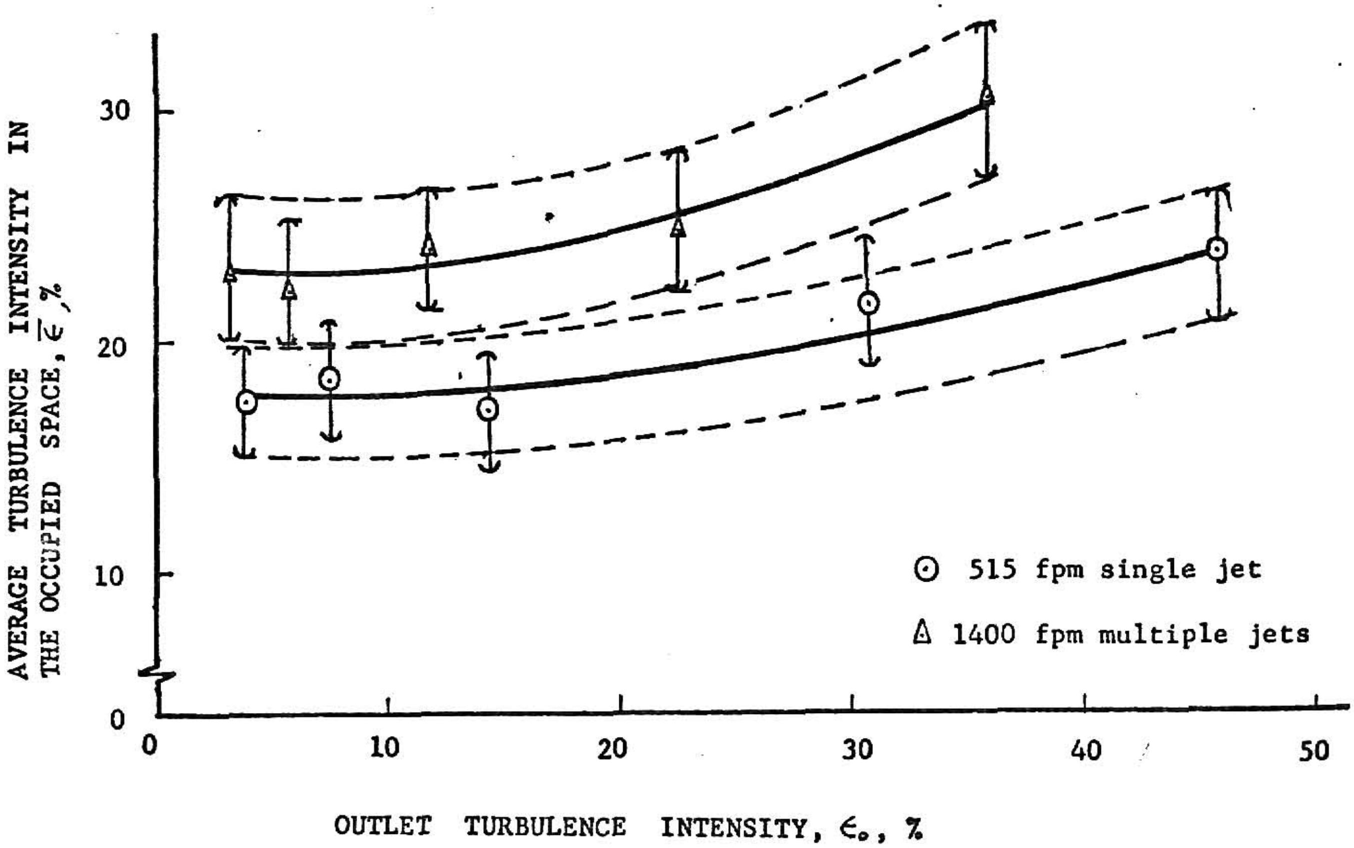

Fig. 39 Average Turbulence Intensity Variations in the Occupied Space for Different Outlet Turbulence Intensities

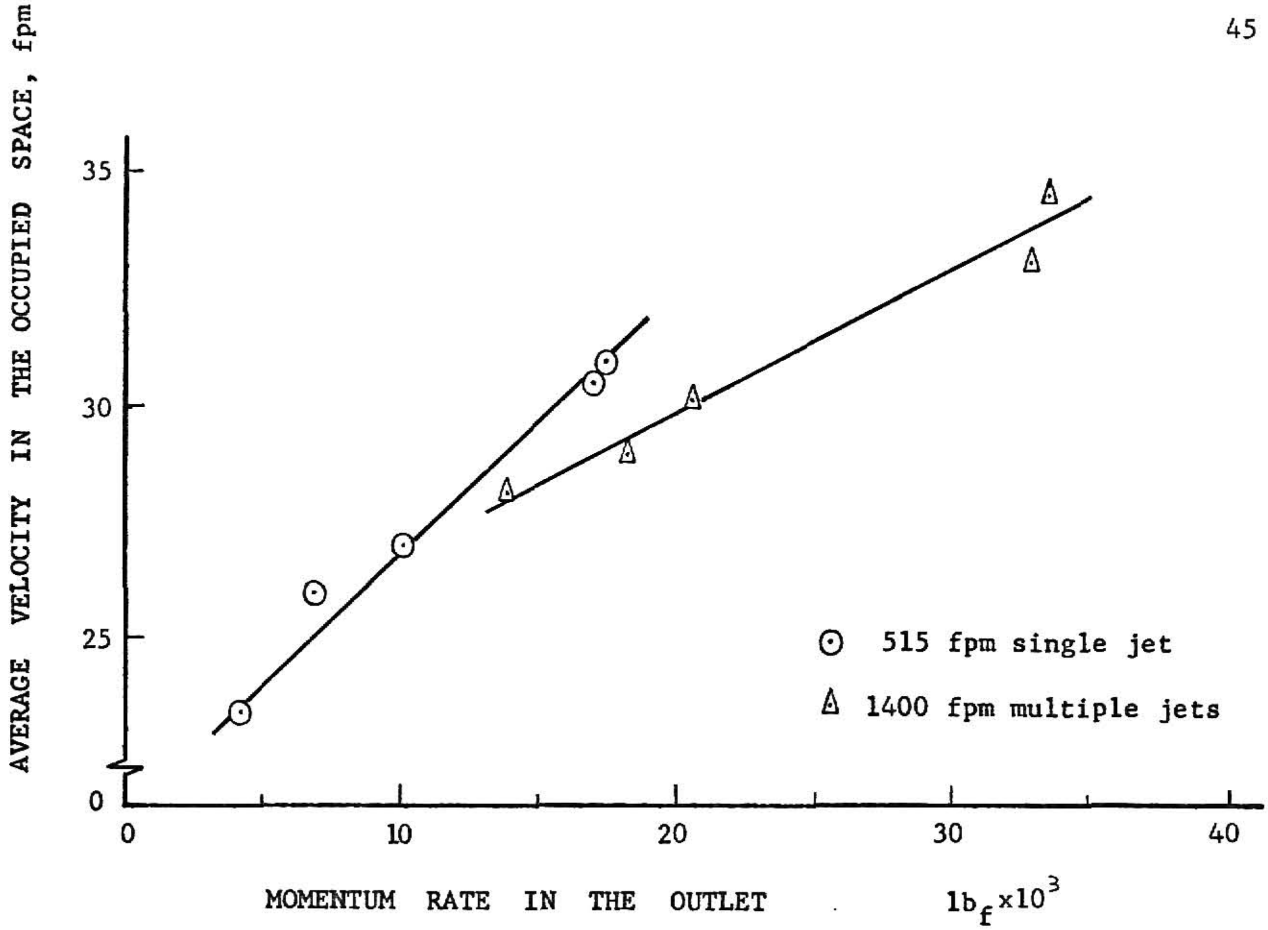

Fig. 40 , Average Velocity Variations in the Occupied Space for Different Outlet Momentum Rates

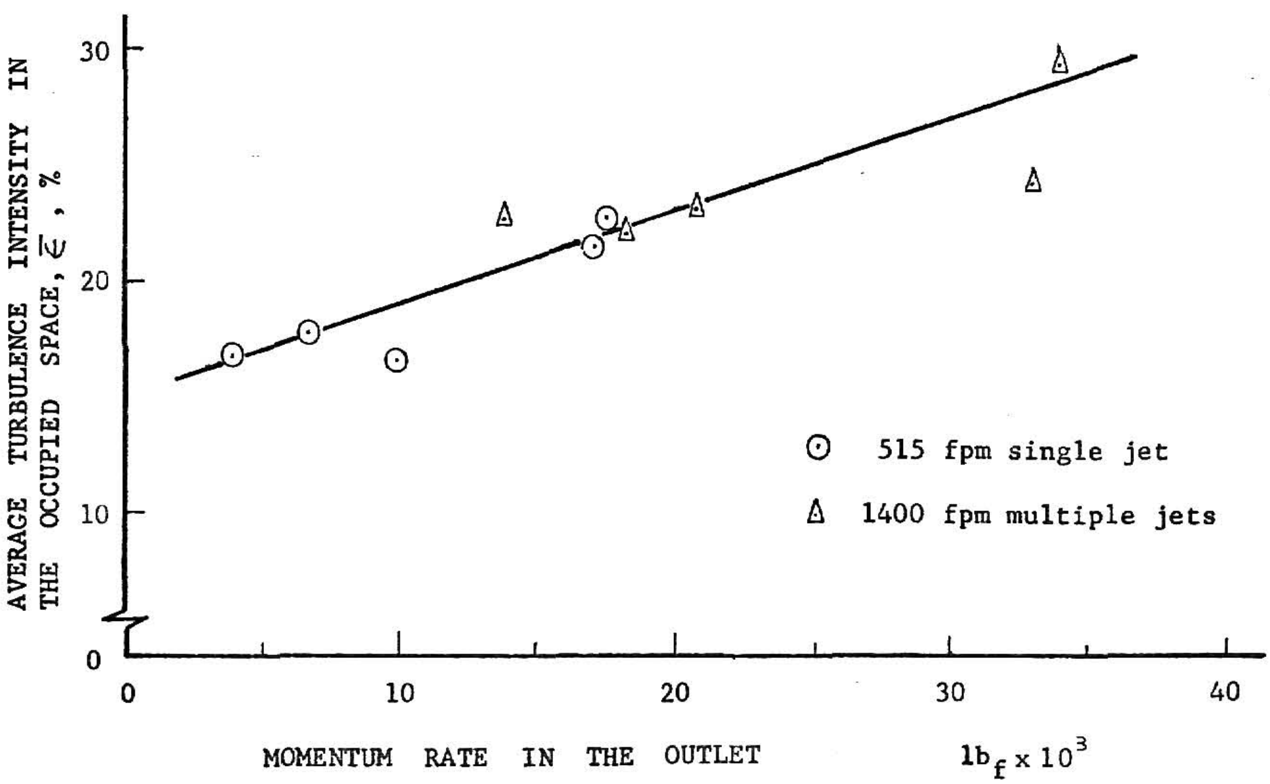

Fig. 41 Average Turbulence Intensity Variations in the Occupied Space for Different Outlet Momentum Rates

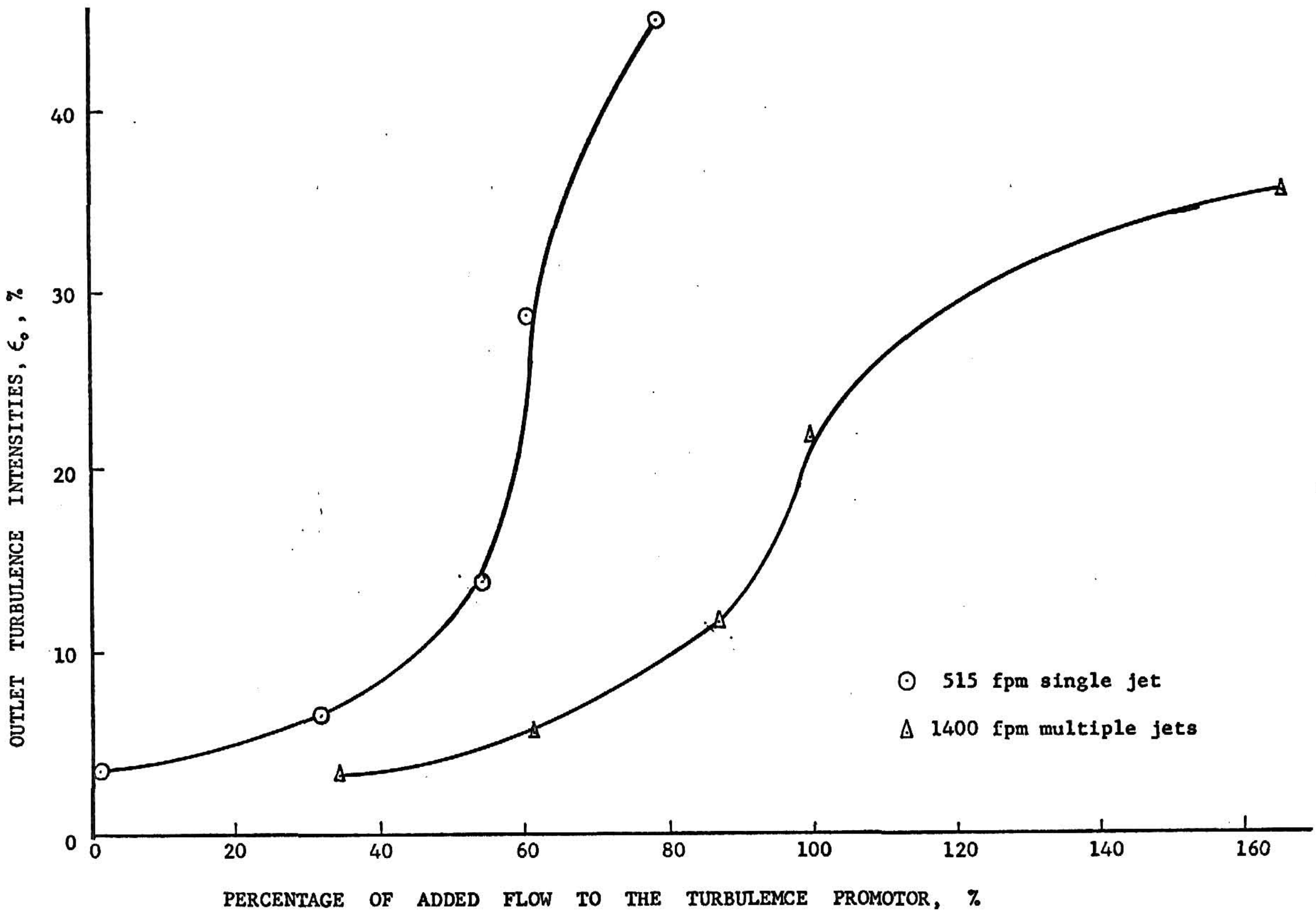

Fig. 42 Outlet Turbulence Intensity Variations by Added Flow to the Turbulence Promotor

REFERENCES

1. H. B. Nottage, J. G. Slaby, and W. P. Gojsza. Isothermal Ventilation--Jet Fundamentals. ASHVE Trans. vol. 58, 1952, p. 107.

2. H. B. Nottage. Turbulence--A Fundamental Frontier in Air Distribution. ASHVE Trans. vol. 55, 1949, p. 193.

3. H. B. Nottage, J. G, Slaby, and W. P. Gojsza. Outlet Turbulence Intensity as a Factor in Isothermal Jet Flow. ASHVE Trans. vol. 58, 1952, p.343.

4. J. Rydberg, and P. Norbadk. Air Distribution and Draft. ASHVE Trans. vol. 55, 1949, p. 225.

5. Alfred Koestel, Philip Hermann, and G. L. Tuve. Air Streams from Perforated Panels. ASHVE Trans. vol. 55, 1949, p. 283.

6. ASHRAE Guide--Fundamentals. 1963, p. 153.

7. P. O. A. L. Davis, M. J. Fisher, and M. J. Barratt. The Characteristics of the Turbulence in the Mixing Region of a Round Jet. Journal of Fluid Mechanics. vol. 15, 1963, p. 337.

8. 1030 Series Constant Temperature Anemometer Instruction Manual. Thermo-Systems Inc. 1965.

9. Shih-I Pai. Fluid Dynamics. New York: D. Van Nostrand Company, Inc. 1954.

10. Hinze. Turbulence. New York: McGraw-Hill Book Company, Inc. 1959.

11. G. L. Tuve. Air Velocity in Ventilating Jets. ASHVE Trans. vol. 59, 1953, p. 261.

12. Alfred Koestel. Computing Temperatures and Velocities in Vertical Jets of Hot or Cold Air. ASHVE Trans. vol. 60, 1954.

13. Alfred Koestel. Pathes of Horizontally Projected Heated and Chilled Air Jets. ASHVE Trans. vol. 61, 1955.

14. R. G. Nevins. Comfortable, Uniform Environment. ASHRAE J. 1961, vol. 3, p. 41.

15. D. W. Nelson, and D J. Stewart. Air Distribution from Side Wall Outlets. ASHVE Trans. vol. 44, 1938, p. 77.

16. Knudsen, and Kats. Fluid Dynamics and Heat Transfer. New York: McGraw-Hill Book Company, Inc. 1958

17. Reference Material sent by R. L. Humphery, Director of Engineering, DISA-S&B, Inc.

18. C. H. Sprague, and R. T. Nash. Introduction to Engineering Experimentation. Blocks 7, 8, 9, 10, 19, and 24

19. Schenck. Theories of Engineering Experimentation. International Text Book Company, Scanton, Pennsylvania

20. G. W. Snedecor. and W. G. Cocbran. Statistical Methods. Chapter 6, Sixth edition, Ames, Iowa: The Iowa State University Press, 1967

21. H. C. Fryer. Concepts and Methods of Experital Statistics. Chapter 6, Boston: Allyn and Bacon, Inc. 1966

22. Specification file for M. E. Lab I, KSU

23. Specification data for DISA 55d35 RMS voltmeter

24. Specification data for TSI 1030 Constant Temperature Anemometer

APPENDIX

UNCERTAINTY ANALYSIS

In evaluating the experimental work performed in this study, the effects of experimental errors upon the results should be considered. This study involved the measurement of air velocities both in a jet and in an occupied space.

The major source of experimental error was a result of the inability to accurately determine low air velocities in the occupied space. This problem arose as a result of the inaccurate linear approximation between the squared bridge output voltage of the anemometer (E_b^2) and the square root of the mean velocity ($\sqrt{\bar{V}}$).

The experimental errors were found to be from ±10% to ±20%, or ±5 fpm for velocities and ±5% for turbulence intensities in the occupied space. These errors would be of smaller magnitude for higher velocities in a jet. An example of the uncertainty analysis at 25 fpm, which is typical of the lowest velocities measured in this study, is given as follows:

<u>Uncertainty in Measuring Room Velocity at 25 fpm</u>

The velocities measured in this study were calculated using a linear equation which was subjected to regression errors:

$$\sqrt{\bar{V}} = a + b\,E_b^2 \qquad (\text{A-1})$$

or,

$$\bar{V} = (\,a + b\,E_b^2\,)^2 \qquad (\text{A-2})$$

where $\bar{V}$ = mean velocity, fpm

a, b = regression constants

E_b = bridge output of the hot-wire anemometer, volt

From the calibration data, a regression line for $\sqrt{\bar{V}}$ versus E_b^2 was

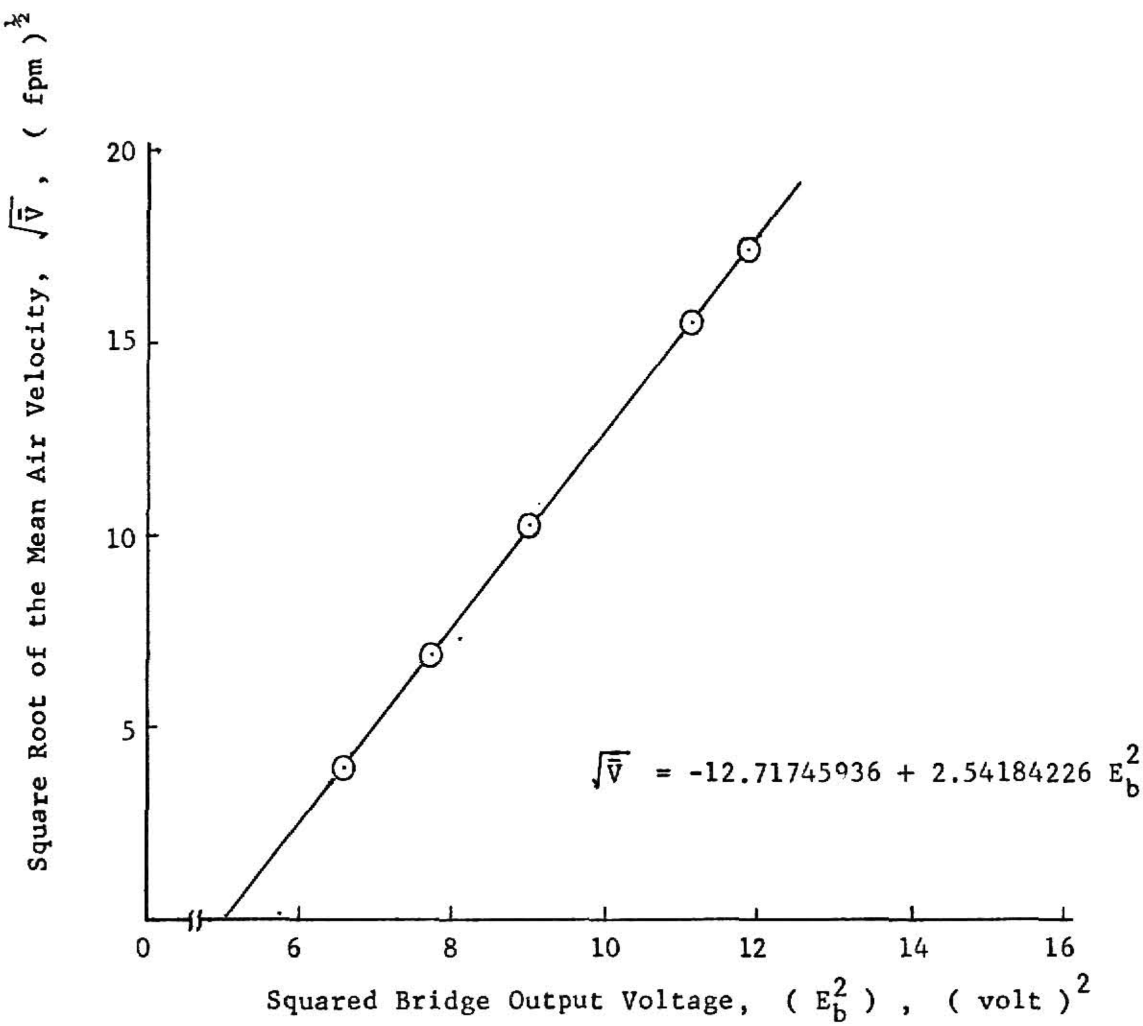

Fig. A-1 Linear Regression of $\sqrt{\bar{V}}$ versus E_b^2

found as shown in Fig. A-1. The calibration data uaed for regression were (6.6, 4.0), (7.7, 6.9), (9.0, 10.2), (11.1, 15.5) and (11.9, 17.5) in which $\overline{E_b{}^2}$ = 9.27, $\sum(E_{b_i}^2 - \overline{E_b{}^2})$ = 19.9.

Through a computer program of linear regression, we have

$$a = - 12.71745936$$

$$b = 2.54184226$$

$$C = 0.99996853$$

$$d^2_{\sqrt{\bar{V}}\cdot E_b{}^2} = 0.00162073$$

where C = correlation coefficient

$d^2_{\sqrt{\bar{V}}\cdot E_b{}^2}$ = an unbiased estimator, with (n-2) degrees of freedom, of the variance of the random errors

The fractional uncertainty in this measurement can be expressed by the following equation[18,19]:

$$\epsilon_{\bar{V}} = \sqrt{S_a{}^2\,\epsilon_a{}^2 + S_b{}^2\,\epsilon_b{}^2 + S_{E_b}^2\,\epsilon_{E_b}^2} \qquad (\text{A-3})$$

where S's denote the sensitivities to $\bar{V}$ and ϵ's the normalized fractional uncertainties. Their values at $\bar{V}$ = 25 fpm are calculated as follows:

S_a:

$$S_a = \frac{\partial \bar{V}}{\partial a}\cdot\frac{a}{\bar{V}} = \frac{2a}{a + b\,E_b^2} = \frac{2a}{\sqrt{\bar{V}}} = \frac{2\,(-12.72)}{5} = -5.09$$

S_b:

$$S_b = \frac{\partial \bar{V}}{\partial b}\cdot\frac{b}{\bar{V}} = \frac{2\,b\,E_b^2}{a + b\,E_b^2} = \frac{2b\,E_b^2}{\sqrt{\bar{V}}} = \frac{2\,(2.54)(6.97)}{5} = 7.08$$

S_{E_b}:

$$S_{E_b} = \frac{\partial \bar{V}}{\partial E_b}\cdot\frac{E_b}{\bar{V}} = \frac{4\,b\,E_b^2}{a + b\,E_b^2} = \frac{4\,b\,E_b^2}{\sqrt{\bar{V}}} = 2\,S_b = 14.16$$

ϵ_a:

From reference[20,21], the variance of the intercept, d_a^2, can be calculated by the equation

$$d_a{}^2 = d^2_{\sqrt{\bar{V}}\cdot E_b^2}\left(\frac{1}{n}\right) \qquad (\text{A-4})$$

where n = number of data

Thus,

$$d_a^2 = 0.00162\left(\frac{1}{5}\right) = 0.000324$$

Or, $d_a = 0.018$

Within the 95% confidence interval, the limit of error is then

$$\pm t_{0.05}\, d_a = \pm 3.182\ (\ 0.018\ ) = \pm 0.0573$$

where $t_{0.05}$ = the tabulated value for t-distribution within the 95% confidence interval

then,

$$\epsilon_a = \frac{t_{0.05}\, d_a}{a} = \frac{0.0573}{-12.72} = 0.451\%$$

ϵ_b:

From reference,[20,21] the variance of the slope, d_b^2, can be calculated by the equation

$$d_b^2 = d^2_{V\,E_b^2}\ \frac{(\ E_{b_i}^2 - \overline{E_b^2}\ )^2}{\Sigma(\ E_{b_i}^2 - \overline{E_b^2}\ )^2} \qquad (\ A\text{-}5\ )$$

$$= 0.00162\ \frac{(\ 6.97 - 9.27\ )^2}{19.9}$$

$$= 0.000431$$

Or,

$$d_b = 0.02075$$

Within the 95% confidence interval, the limit of error is then

$$\pm t_{0.05}\, d_b = \pm 3.182\ (\ 0.02075\ ) = 0.066$$

then,

$$\epsilon_b = \frac{t_{0.05}\, d_b}{b} = \frac{0.066}{2.54} = 2.595\%$$

ϵ_{E_b}:

According to the experimental data for a velocity of 25 fpm: $E_b^2 = 6.97$, or, $E_b = 2.64$, and from the manufacturer's specifications,[22] the accuracy of E_b is

$\pm$ (0.1% of reading + 0.1% of full scale)

then, we have

$$\epsilon_{E_b} = \frac{1}{E_b} \cdot \sqrt{(0.1)^2 (2.64)^2 + (0.1)^2 (20)^2}$$

$$= 0.758\%$$

Substituting these values in equation (A-3), we obtain

$$\epsilon_{V=25fpm} = \pm 21.4\%, \quad \text{or,} \quad \pm 5 \text{ fpm}$$

Through the same procedure, the velocity uncertainty at $\bar{V}$ = 50 fpm was found to be

$$\epsilon_{\bar{V}=50fpm} = \pm 10.2\%, \quad \text{or,} \quad \pm 5 \text{ fpm}$$

Uncertainty in Measuring Room Turbulence Intensity:

The turbulence intensity (I) was calculated by the equation

$$I = \frac{\sqrt{\overline{v'^2}}}{\bar{V}} = \frac{4 V_{rms} E_b}{E_b^2 - e} \qquad (A-6)$$

where V_{rms} = reading from the root-mean-squared voltmeter, volt

e = intercept on E_b^2 axis

The fractional uncertainty for measuring turbulence intensity can be expressed by the following equation[18,19]:

$$\epsilon_I = \sqrt{S_{V_{rms}}^2 \epsilon_{V_{rms}}^2 + S_{E_b}^2 \epsilon_{E_b}^2 + S_e^2 \epsilon_e^2} \qquad (A-7)$$

where S's denote sensitivities to I and ϵ's the normalized fractional uncertainties, their values at $\bar{V}$ = 25 fpm are calculated as follows:

$$S_{V_{rms}} = \frac{\partial I}{\partial V_{rms}} \cdot \frac{V_{rms}}{I} = 1$$

$$S_{E_b} = \frac{\partial I}{\partial E_b} \cdot \frac{E_b}{I} = -\frac{E_b^2 + e}{E_b^2 - e} = -\frac{6.97 + 5.0}{6.97 - 5.0} = -6.075$$

$$S_e = \frac{\partial I}{\partial e} \cdot \frac{e}{I} = \frac{e}{E_b^2 - e} = \frac{5.0}{6.97 - 5.0} = 2.605$$

According to the experimental data, a typical value of V_{rms} in the occupied space is 0.03 volt, and from the manufacturer's specifications,[22,23] the accuracy of the V_{rms} is

$\pm$ (1% of output + 0.1% of reading + 0.2% of full scale)

then, we have

$$\epsilon_{V_{rms}} = \frac{1}{V_{rms}} \sqrt{(1)^2 (0.03)^2 + (0.1)^2 (0.03)^2 + (0.2)^2 (0.2)^2} \ \%$$

$$= 1.66\%$$

From the previous section, we have

$$\epsilon_{E_b} = 0.758\%$$

$$\epsilon_e = \epsilon_a = 0.451\%$$

Substituting these values into equation (A-7), we obtain

$$\epsilon_{I}\Big|_{\bar{V}=25fpm} = \pm 5.04\%$$

Through the same procedure, the uncertainty of turbulence intensity at $\bar{V}$ = 50 fpm was found to be

$$\epsilon_{I}\Big|_{\bar{V}=50fpm} = \pm 3.89\%$$

ACKNOWLEDGEMENTS

The author wishes to express his gratitude to Dr. Ralph G. Nevins, major professor, for his suggestion of this exploratory investigation and his guidance in the preparation of this thesis. Appreciation is also expressed to Dr. Paul L. Miller for his valuable comments, and to Dr. John E. Kipp for his guidance in the labratory instruments. Thanks are due also to Mrs. Hui-Min Hsu for her typing and drawing of the manuscript.

EFFECTS OF OUTLET TURBULENCE INTENSITY UPON AIR DISTRIBUTION

by

SUNG-NAN HSU

B. S., Taiwan Cheng Kung University, 1967

AN ABSTRACT OF A MASTER'S THESIS

submitted in partial fulfillment of the

requirements for the degree

MASTER OF SCIENCE

Department of Mechanical Engineering

KANSAS STATE UNIVERSITY

Manhattan, Kansas

1973

ABSTRACT

The purpose of this research was to investigate the effects of the outlet turbulence intensity upon the air velocities and turbulence intensities both at the center-line of the jet and in the occupied space.

A model space (12 in x 12 in x 44 in) was used for this study. Five tests with different outlet turbulence intensities were conducted with a 515 fpm single jet and a 1400 fpm multiple jets respectively. Changing of the outlet turbulence intensity was made by using a turbulence promoter.

The outlet turbulence intensity was found to be a more important variable in decreasing the throw of the single jet than the multiple jets, mainly because the latter would have higher outlet velocity.

The turbulence intensities in the occupied space were random and unsteady. A statistical analysis of the experimental data indicates that for a outlet turbulence intensity less than 20%, no significant effect was detected upon the turbulence level in the occupied space.